Development of Adsorbents for Phosphate Removal from Aqueous Solution

May 2013

Shengjiong YANG

Development of Adsorbents for Phosphate Removal from Aqueous Solution

A Dissertation Submitted to the Graduate School of Life and Environmental Sciences,

The University of Tsukuba in Partial Fulfillment of the Requirements

For the Degree of Doctor of Environmental Studies

(Doctoral Program in Sustainable Environmental Studies)

Shengjiong YANG

Abstract

Phosphorus is an essential nutrient element in water environment for the growth of aquatic plants and algae. A large amount of phosphorus in water body is often responsible for algal bloom and eutrophication, which causes many environmental problems. Further, phosphorus is also an un-renewable recourse which is necessary in food production for human beings. The reserves of phosphorus in the world will deplete in 50 - 100 years. Thus, the removal of phosphors in water body and recycling of phosphorus from P wasted water is necessary and urgent. The objective of this research is to develop a high capacity novel phosphate adsorbent for phosphate removal and recycling from aqueous solution. Three parts of work have been conducted.

1. Kanuma mud had been selected as basic material for further material development. Laboratory-scale batch experiments were conducted to investigate the efficiency of Kanuma mud for phosphate removal from aqueous solution. The adsorption isotherms, kinetics, desorption rate and some factors such as temperature, pH and dosage were investigated. The phosphate adsorption results fitted the Freundlich isotherm model very well, and the adsorption process was an exothermic reaction which could be described by a pseudo-second-order kinetic model. A maximum phosphate adsorption capacity of 2.13 mg g^{-1} was achieved under the condition of 4 g L^{-1} dosage and 50 mg L^{-1} initial concentration, and the effective phosphate uptake step could be attained in 90 min. The adsorption performance was the best at pH 6, and the adsorbed phosphate on the Kanuma mud could be hardly

desorbed in deionized water. These results showed that Kanuma mud processed great potential for using as an absorbent for phosphate removal from aqueous solution.

2. A novel tablet porous material (TPM) was further developed from Kanuma mud (K - mud), corn starch and calcium oxide. Laboratory-scale batch experiments were conducted to evaluate the phosphate adsorption capacity of TPM from aqueous solution. The adsorption isotherms, adsorption kinetics, phosphate recycling and major factors such as temperature, pH and dosage were investigated. The phosphate adsorption results fitted the Freundlich isotherm model very well, and the adsorption process was an endothermic and spontaneous reaction which could be described by a pseudo-second-order kinetic model. The maximum phosphate adsorption capacity was 4.39 mg g^{-1} under the condition of 4 g L^{-1} dosage and initial pH of 7. Its equilibrium could be attained in 2 h. The solution pH had little effect on TPM phosphate removal when pH varied from 5.0 to 9.0. 70.29% of adsorbed phosphate could be recycled when 0.2 mol L^{-1} HCl were used as eluant, and the present developed TPM could be recovered and reused for 5 times. The adsorption capacity would be continuously decreased with the increase of elute cycles. The adsorption capacity was 1.316 mg g^{-1} for raw TPM and decreased to 0.466 mg g^{-1} after 5 cycles. This novel developed TPM is a promising adsorbent than other clay mineral materials for phosphate removal from wastewater.

3. The adsorption performance of developed TPM was further enhanced through an electrochemical surface modification (ESM) method. Laboratory-scale batch experiments were conducted to compare the phosphate adsorption capacity of TPM and ESM modified TPM (ECTPM) from aqueous solution. The adsorption isotherms, adsorption kinetics and major factors such as temperature and pH were investigated. The phosphate adsorption results fitted the Freundlich isotherm model very well, and the adsorption process was an endothermic and spontaneous reaction which could be described by a pseudo-second-order kinetic model. Under the condition of 4 g L^{-1} dosage and initial pH of 7, the maximum phosphate adsorption capacity was 3.61 mg g^{-1} onto TPM and 5.36 mg g^{-1} onto ECTPM, respectively, and the equilibrium could be attained in 2 h. The solution pH had little effect on TPM phosphate removal when pH varied from 5.0 to 9.0. ECTPM and TPM are of high selectivity on phosphate adsorption. This newly developed ECTPM is also promising than other clay mineral materials for phosphate adsorption from wastewater.

On the whole, Kanuma mud and the developed TPM could be used as effective phosphate adsorbent from aqueous solution. In addition, the new developed electrochemical surface modification (ESM) method could be used for adsorbent surface modification.

Contents

Chapter 1 Introduction

1.1 The world's water resources & wastewater treatment

During the past century, the world population tripled, the use of water increased and followed the world population. In human life and industrial activities, agriculture irrigation accounts for 70% of global water withdrawals, and municipal accounts and industry usage accounts for 30% [1]. The increased population brings about many environmental problems, about 50% of wetland in the world gave disappeared during the past century [2]; some rivers might dry up and no longer reach the sea [3], and result in the extinction of freshwater aquatic animals. Further, many important groundwater aquifers are being mined leading to water table dropping, and some of them were damaged by permanent salinization. It is estimated that water use will increase by about 50% in the coming 30 years [1]. Approximately 3.7 billion (about half of the world population) people were estimated to live under severe water shortage condition, especially in Africa and Middle East (in which about 1.1 billion people can not access to safe drinking water; and 2.6 billion people lack access to improved sanitation facilities) [4].

Most nations confront two major water resources challenges. Firstly, all countries face challenges in regulation and laws developing to manage water resources in an economically productive, socially acceptable and environmentally sustainable way. Secondly, all countries have difficulties in water infrastructure maintaining and developing for an appropriate stock of water resources. The cost of water infrastructure will rapidly rise up in many nations due to these challenges. The World Bank [5] reported that the cost of water or future project is 2 - 3 times higher than that

of the previous one. The Water Infrastructure Network (WIN) reported that the annual investment gap for municipal wastewater and drinking water system during 2000 - 2020 would reach $24.7 billion [6], and over the 20-year period, $940 billion is required for wastewater and drinking water investment [7]. Further, irrigation is a high volume in water use. The growth of world population would extent the water use in irrigation, and burdens the water shortage.

In the present world, approximately 150 - 200 million hectares of land are drained up, including 100 - 150 million hectares of rain-fed land and approximately 50 million hectares of irrigated land. This part of land produced 10 - 15% of global food [8]. Drainage developments are desired to improve agricultural productivity. The global irrigated land increased by more than 2% per year in the 1960s and 1970s, and decreased to 1.6% in the 1980s [9]. Thus, it can be concluded that the increase usage of groundwater used in irrigating is foreseeable because of greater certainty of supply, advances in technology in many instances, government subsidies for power and pump installation. At present, the increasing use of groundwater has led to the overexploitation of groundwater resources in some arid and semiarid regions, where water tables are falling. Consequently, proper use of water for irrigation and drainage is essential for sustainable water resources management.

On the other hand, continuous growths of population and industrialization have resulted in the degradation of various ecosystem on which human life relies, such as ocean and river. These systems are always polluted by discharging inadequately treated wastewater. Many pollutants may be easily removed before discharge into the

environment, but the treatment became more and more difficult after the pollutants dispersed into the environment. To realize the sustainable water use and relief the burden on aquatic environment, wastewater treatment should be considered seriously. At present, diverse contaminants are produced in human life and industrial activities and discharged into aquatic environment. In municipal wastewater, large amount of organics, N and P are existed, N and P will also exist in low concentration either the wastewater were treated. This part of N and P would lead to many environmental problems when they are accumulated in the environment. Thus, the treatment of N, P and organics in wastewater is urgent and necessary to relieve water shortage and realize wastewater recycling to a certain extend.

1.2 Phosphorus issues

Phosphorus is an essential nutrient element in food production, playing a major role in agricultural and industrial development. In the 21st century, the world population is about to 7 billion [10], the requirement of phosphorus in agriculture will largely increase. Further, phosphorus is also used in many other fields, such as production of automobile battery, surface additive in solar LED panel production and digital device product (television, camera, etc.). In addition, the development of bio-field is based on sufficient phosphorus supply, or it could not advance develop if the shortage happened.

At present, phosphorus is always obtained from finite phosphorus-mineral. However, the reserve of phosphorus mineral is limited. The 85% of phosphorus

mineral reserve is centered in 4 nations, including Mongolia, China, USA and South Africa [11]. Actually, the phosphorus resources in China and USA have begun to be exhausted. With the time going on, the phosphorus would be only supplied by Mongolia. Since 1997, the export of phosphorus mineral from USA has been terminated. The world phosphorus utilization would be threatened if other nations follow this step. Japan is the 8^{th} phosphorus consumption nation in the world, all the consumed phosphorus in Japan was imported from other nations. However, with the phosphorus resources self-protection followed up, the import of phosphorus would be increasingly difficult. The food self-supporting and development of biomass techniques would largely limit. Further, to 2050, the world population will achieve 9 billion [11]; the food production to support such a large number of population should be taken seriously. On the other hand, wider utilization of P in human life and industrial activities enhances the nutrient element load when P-waste is discharged into water bodies without any treatment, resulting in eutrophication and red tide in lake, reservoirs and ocean. In most cases, phosphorus is the limiting factor in eutrophication [12]. The eutrophication resulted in many problems, such as disturbing aquatic ecosystem, over consumption of dissolved oxygen and aesthetics problems. In addition, some environmental toxicants like microsystin will be produced when eutrophication happened; these substances would be accumulated in the bodies of aquatic animals and finally affect the health of human beings. Thus, phosphorus contamination should be avoided. To protect environment and surface water, the discharge concentration of total phosphorus to environment was limited by many

countries, but the development and utilization of phosphorus removal techniques was different between developed countries and developing countries because of the economic level and investigation. Thus, the academic exchange between different countries should be intensified to save environment between different countries. Also, the issue on phosphate recycling should also be considered.

1.3 Phosphorus removal and recycling techniques

In the past decades, the development of technology for phosphorus removal offers the chance for phosphorus controlling in water environment. The development of phosphorus removal technologies was started in the 1950s to reduce the content of phosphorus entering surface waters [13]. It was initially achieved by chemical precipitation [14-16], which is also a leading method at present. However more recently, biological [17, 18], crystallization [19, 20] and adsorption [21, 22]methods have been established and well developed.

1.3.1 Chemical precipitation

The widespread uses of chemical precipitation for P removal in wastewater treatment were started since the 1950s to control the eutrophication in water bodies. It was developed in many countries at an accelerating rate due to easy operation.

Chemical precipitation is a physical-chemical process. When the divalent/trivalent metal salts were dosed into wastewater, an insoluble metal-phosphate precipitation would be caused. Iron and aluminum were always used as the effective precipitants [23, 24]. The flow chart of traditional chemical precipitation is shown in Figure 1.1.

The phosphorus is removed through primary sedimentation and secondary precipitation in the chemical precipitation process. It typically produces phosphorus bound as a metal salt within the wasted sludge and separated from liquid phase. The P-sludge is also valuable when disposed to agriculture. Although a high quality effluent can be achieved, chemical precipitation is not generally favored because of its high cost and further treatment needed.

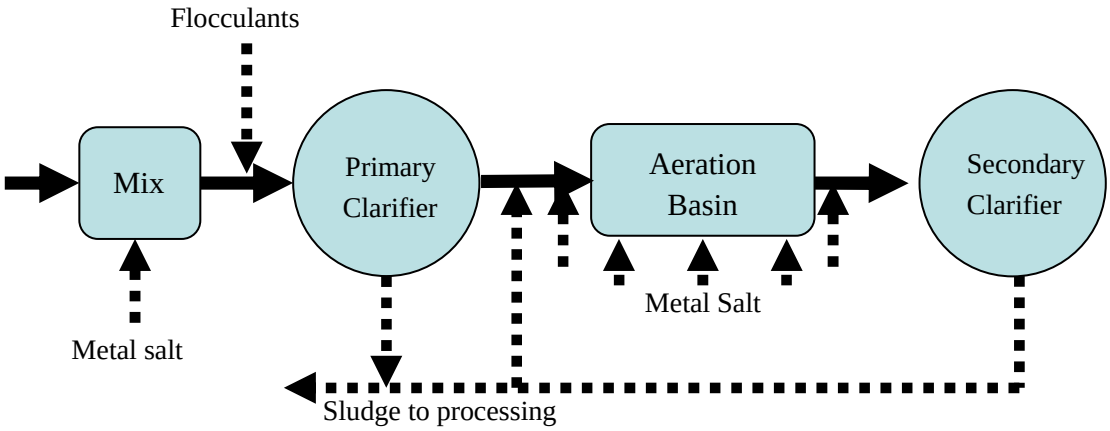

Figure 1.1. The flow chart of P removal by chemical precipitation [13].

1.3.2 Biological removal

The biological phosphorus removal techniques were developed in the 1950s. The researchers found that activated sludge could over take up phosphorus for normal biomass growth under certain conditions [25, 26]. Based on this observation, a number of processes have been developed and the technical system is now firmly established and serving large populations in the world. The advantage of this technique is obvious (low cost, no chemical material required). However, more complicated plants and configurations are necessary [27] (Figure 1.2). Biological P uptake is achieved through the following processes in the system: a) the phosphorus is released into the wastewater by microorganisms, b) in the subsequent aerobic stage, the released and extra phosphorus will be taken up by PAOs (phosphate-accumulating organisms). The sludge which is rich in phosphorus would be produced and discharged from the system, resulting in phosphorus removal from the treatment system.

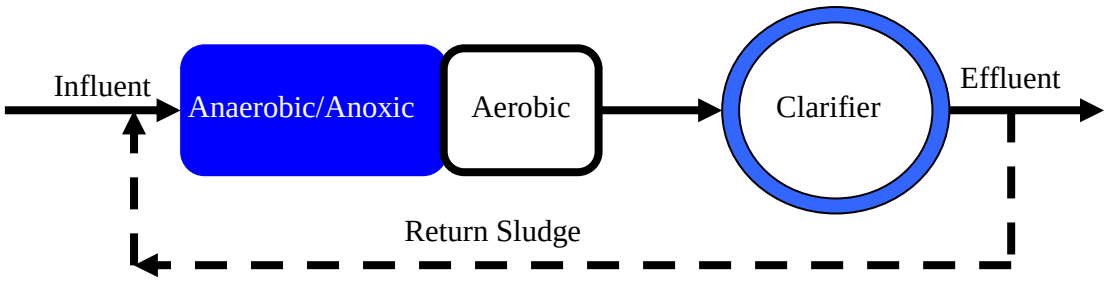

Figure 1.2. The flow chart for basic biological P removal process.

1.3.3 Crystallization

Crystallization was developed in the 1970s. The recycling of phosphorus from liquid phase, sewage sludge or sewage sludge ash can be achieved through crystallization [28]. In this process, the phosphorus was always pretreated through microorganisms to transfer phosphorus into phosphate, then in which phosphate could be removed through HAP (hydroxyapatite) production process, in which $Ca_{10}(OH)_2(PO_4)_6$ on the surface of seed crystal could be applied to the removal of phosphate from liquid [29]. The removed phosphate from liquid could be used as phosphorus resources again. Many attempts have been tried to test the applicability of the phosphorus crystallization process as a phosphorus recovery system for phosphate removal and recycling in wastewater [30-33]. The principal chemical reaction for the crystallization of HAP is as follows [34]:

$$10Ca^{2+} + 6PO_4^{3-} + 2OH^- \rightarrow Ca_{10}(OH)_2(PO_4)_6 \quad (1.1)$$

The traditional phosphorus crystallization process could be explained by Figure 1.3.

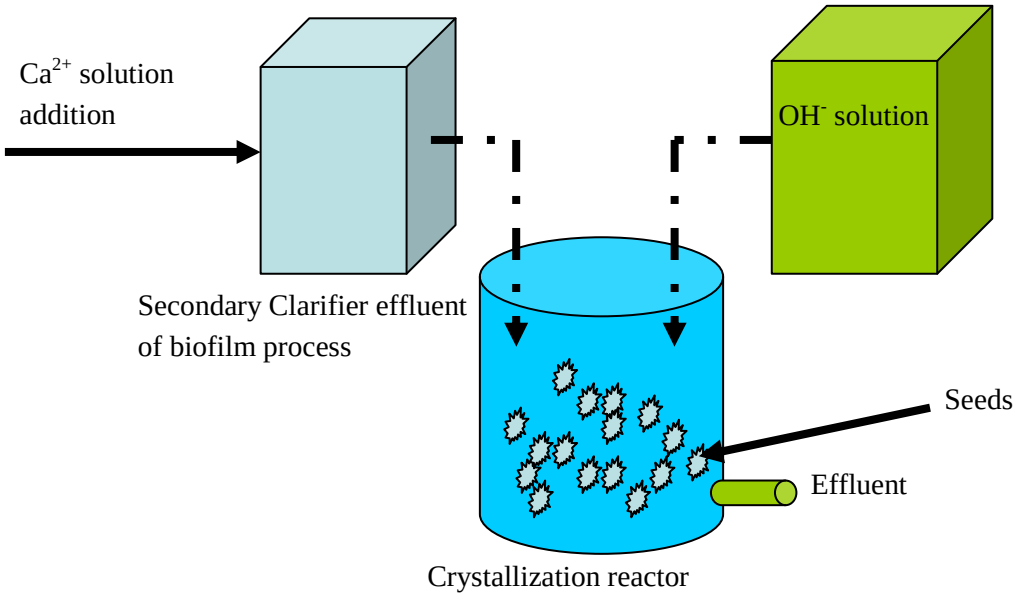

Figure 1.3. The schematic diagram of phosphorus crystallization process [29].

1.3.4 Adsorption

Adsorption enables the separation of selected compounds from liquid. Compared to alternative techniques, adsorption is attractive for its relative simplicity of design, easy operation, insensitive to toxic substance, ease regeneration and low cost.

In the past decades, many researches were attempted for different pollutant removal; it has been widely used in many fields, such as treatment of dyeing and decolor wastewater [35], purification of drinking water [36], refinement of important content in component [37] and so on. On the other hand, the theoretical research of adsorption is slower than its application in practice. In the present adsorption studies, the research focus is mainly concentrated on the following aspects:

i. New application development (environmental protection, material science, energy development and refinement).
ii. Exploration of theory and impact factors (isotherms development etc.)
iii. Investigation of thermodynamics and kinetics (to figure out the driving force).
iv. Mechanisms investigation.

Based on this situation, the adsorption technique have been widely developed for environment protection and pollutants removal, such as phenol [38], nitrate [39], methylene [40], dyes [41], protein [42], arsenic [43], chromium [44] and so on (Table 1.1). Also, the phosphorus as a traditional pollutant can also be removed through adsorption method. With the development of adsorption method, new adsorbents were appeared at the same time, such as activated carbon [45, 46], zeolite [46], resin [47], carbon fiber [48], clay mineral [49-51], etc. Among those adsorbents, clay minerals

have been proved to be effective and low cost ones. For phosphate removal, diverse clay minerals have been used as adsorbents (Table 1.2), including alunite [52], palygorskites [53], bentonites [54], dolomite [21], kaolinite [50, 55], goethite [55] and so on. The phosphorus can be removed through static adsorption, chemical precipitation and chemical adsorption due to the complex components in the clay mineral. The clay mineral adsorbents exhibit effective removal efficiency, but still drawbacks, such as low capacity, low availability in Japan.

`

Table 1.1 The application of adsorbent/adsorption in waste & wastewater treatment.

Adsorbate	Adsorbent	Capacity (mg g^{-1})	Data source
Phenol	Activated carbon fibers	1.09-2.21	[38]
Nitrate	Double hydroxides	1.60-4.98	[39]
Methylene	Cotton stalk	147.06-222.22	[40]
Dye	Sepiolite	-	[41]
Protein	Bioactive glass	-	[42]
Chromium	Dolomite	5.67-10.01	[44]

Table 1.2 The clay minerals used for phosphate adsorption.

Clay	Capacity (mg g^{-1})	BET surface area (m^2 g^{-1})	Data Source
Alunite	118	29-148	[52]
Palygorskites	3.73-8.31	287-342	[53]
Bentonites	9.47-10.54	39.30	[54]
Dolomite	8.20-13.50	0.14	[21]
Kaolinite	5.05-17.89	-	[50]
Goethite	-	47.6	[55]

1.4 Originalities and objectives

In this field, the researches of adsorption method are mainly concentrated on material development. In this study, an attempt was tried to develop a new material for phosphorus removal and further for phosphorus recycling. The originalities of this research were followed：

i. The basic material (Kanuma mud) used for phosphorus adsorption is unique in Japan and few research on phosphorus removal is reported.

ii. The Kanuma mud is firstly developed to granular adsorbent with enhanced phosphorus removal efficiency.

iii. A new modification method is applied to further enhance the phosphate removal capacity of the newly developed granular adsorbent.

1.5 The contents and framework of this research

The results of this research were grouped into three parts which were presented chapter by chapter.

i. In the first part of this research, the selection of optimum basic material suitable for phosphorus removal was conducted. Its phosphorus removal capacity was investigated. The adsorption isotherm, kinetics, effect of pH and temperature was measured. The optimum removal condition was obtained.

ii. In the second part of this research, the selected basic material was used to develop a new granular phosphorus adsorbent. The phosphorus removal capacity of the developed granule was investigated. The adsorption isotherm,

kinetics, thermodynamics, and effect of pH were measured. The optimum removal condition was confirmed. In addition, the phosphorus recycling was also investigated in this part.

iii. In the third part of this research, the developed granular material was surface modified through a novel surface modification process. The phosphorus removal capacity of surface modified granule was investigated. The adsorption isotherm, kinetics, thermodynamics, effect of pH was measured. The optimum removal condition was confirmed.

The experimental framework is briefly illustrated in Figure 1.5

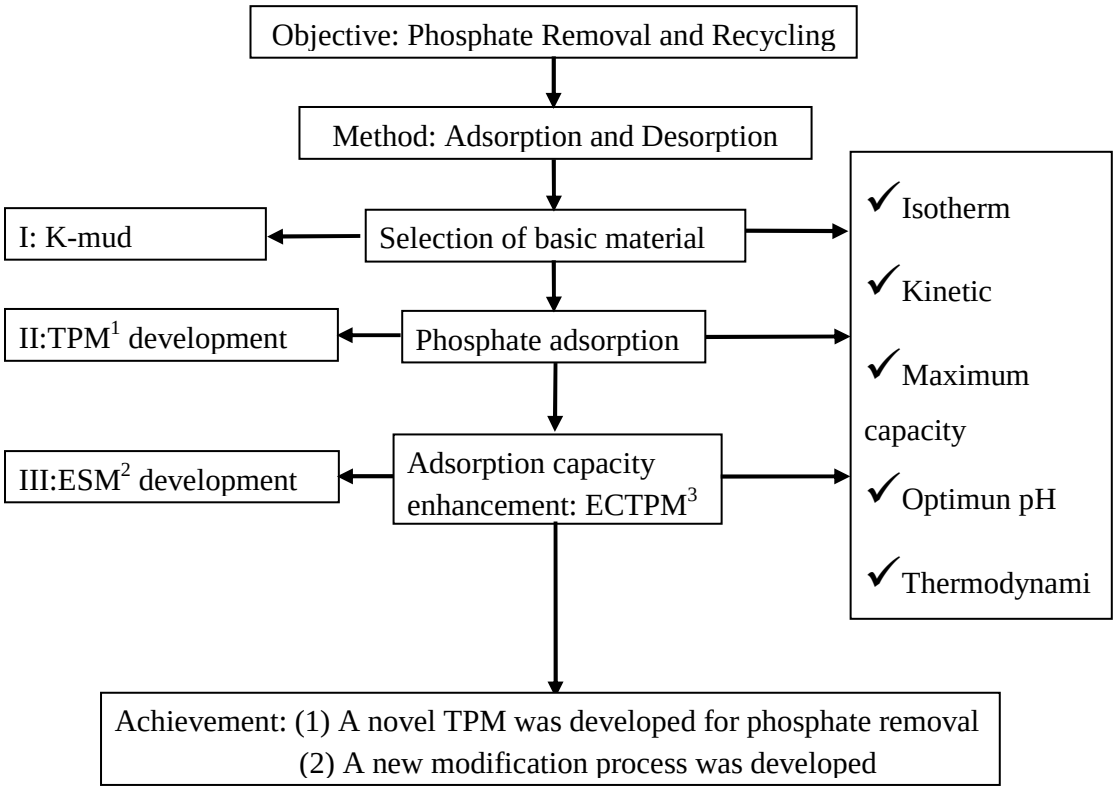

Figure 1.5. The framework of this research.

K-mud: Kanuma mud; TPM: tablet porous materials; ESM: electrochemical surface modification process; ECTPM: ESM modified TPM.

Chapter 2 Phosphate adsorption from aqueous solution using Kanuma mud

2.1 Introduction

Phosphorus is an important nutrient element in surface water environments for the growth of aquatic plants and algae [56]. The majority of phosphorus used in living and production activities of human beings is discharged into water environment finally through natural phosphorus cycle. An over loading of phosphorus in water environment is often responsible for algal bloom and eutrophication [57-59], especially in lakes, coastal areas and reservoirs, causing many environmental damages such as esthetic problem [60], dissolved oxygen (DO) decrease and destroy aquatic ecosystems leading to death of aquatic animals [61]. In addition, environmental toxin such as microsystin would be produced in eutrophication process. The microsystin enriched in the body of aquatic animals and transferred into human body led to hepatocellular carcinoma [62]. Thus, the regulation limits of phosphors discharging were performed in many nations to prevent those problems.

In the past decades, phosphorus removal from wastewater has been extensively developed, including precipitation through chemical methods [63], activated sludge [64], ion exchange [65], phosphate crystallization [66], etc. Those techniques achieved effective efficiency of phosphorus removal, but still drawbacks, such as high cost, low efficiency and complicated operation. On the contrary, adsorption method is increasingly used in many researches related with phosphorus removal because of its high efficiency and convenient operation. Diverse absorbents have been used for

phosphorus removal, such as peat [67], alunite [52], palygorskite [53], red mud [68], mussel shells [57], dolomite [21], palm waste [69], etc.

Kanuma mud, a kind of inorganic volcano geomaterial, is very abundant in Japan especially in Kanuma city (Located in Tochigi prefecture). It is widely used in agriculture and horticulture. Kanuma mud has functional physical and chemical abilities such as high permeability, water retention ability and porosity. It has been used for fluoride removal from aqueous [70], but few studies can be found on its phosphorus removal capacity through adsorption methods using Kanuma mud.

Therefore, in this study, an attempt was tried to investigate the efficiency of phosphorus removal through Kanuma mud from polluted aqueous solutions. The adsorption isotherms, adsorption kinetics, effect of temperature on adsorption, effect of pH on adsorption, and desorption rate were discussed.

2.2 Experimental

2.2.1 Preparation of the phosphate adsorbent

The absorbents used in present study were bought from the Makino Store, Kiyosu, Japan. It was manually smashed and sieved, and the particles less than 300 μm were selected. The absorbents were washed by distilled water for five times and dried at temperature of 60 ^{o}C. Thermal treatments were performed at temperature of 120 ^{o}C last for 24 h (dewater) after washing. The dewatered Kanuma mud was examined by X-ray diffractometer (XRD, RINT2200, Rigaku, Japan), energy dispersive X-Ray Spectroscopy and scanning electron microscope (SEM XL40 series philips, Holland)

to obtain its physical, chemical and surface characteristics; Brunauer-Emmett-Teller (BET) specific surface area was obtained by a analysis device (Coulter SA3100, US) using the He - N_2 method. All the equilibrium phosphate concentration was analyzed with the ascorbic acid method (4500-P E) [71].

2.2.2 Adsorption experiments

Phosphate adsorption isotherm study was carried out. An amount of 0.5 g prepared adsorbents was added in a test tube (50 mL) with series initial concentrations of phosphate (anhydrous KH_2PO_4, analytical grade). The concentrations were ranging from 5 to 50 mg L^{-1}, respectively. The test tubes were set in a thermostat at temperature of 25 ± 1 ^oC. Centrifugations were performed at 5000 rpm for 5 min after equilibrium. The supernatant liquid was used for phosphate concentration analysis after filtered through a 0.45 μm membrane filter. The adsorption isotherms can be obtained by fitting the experimental data to the related isotherms.

2.2.3 Kinetic experiments and effect of different initial concentration

Phosphate adsorption kinetic studies were conducted in a thermostat at temperature of 25 ± 1 ^oC. An amount of 1 g samples were put into a series of test tubes (50 mL) with the concentration of 10, 15 and 20 mg L^{-1} phosphate solution (anhydrous KH_2PO_4, analytical grade). The time intervals were 5, 10, 20, 30, 90, 120, 180, 300, 420, 600, 840, 1020, 1320 and 1440 min, respectively. Centrifugations were

performed immediately each time, and the resultant supernatants were used for phosphate determination after filtered through a 0.45 μm membrane filter.

2.2.4 Effect of pH on phosphate adsorption

Twenty five milliliter phosphate solutions (10 mg L^{-1}) were added in 12 test tubes set in a thermostat at a temperature of 25 ± 1 ^{o}C, and 0.5 g of adsorbent was added to each tube. Different amount of 0.1 M HCl and NaOH were used to adjust pH value range from 1.5 and 2 to 12, all the test tubes were capped after dosing to avoid evaporation, and the phosphate concentration were determined after 24 h.

2.2.5 Effect of temperature on phosphate adsorption

The effect of temperature on phosphate adsorption was investigated at fixed amount of adsorbent and initial concentration of 10 mg L^{-1}. An amount of 1 g adsorbent was added in each test tube with 50 mL phosphate solution. The pH of the suspension was adjusted to 5.8. Then the test tubes with the content were capped and set in a temperature thermostat at different temperature (5, 25 and 35 ^{o}C). At the end of 24 h treatment, centrifugations were performed at 5000 rpm for 5 min after equilibrium. Supernatants were obtained and filtered through a 0.45 μm membrane filter for phosphate concentration analyzing.

2.2.6 Desorption studies

The phosphate desorption studies of P-adsorbed Kanuma mud were also investigated. Amounts of 1 g prepared adsorbent were added in a test tube (50 mL) at

different initial concentration of phosphate (anhydrous KH_2PO_4, analytical grade). The concentrations were 1, 2, 5, 10 and 15 mg L^{-1}, respectively. The test tubes were set in a thermostat at a temperature of 25 ± 1 ^oC. The equilibrium concentrations of phosphate adsorption were determined after 24 h. The phosphate adsorbed absorbent was filtered and dried for 2 h at 60 ^oC, and then added into 5 test tubes with 50 mL distilled water, respectively. All the test tubes were shaken at 200 rpm in a temperature controlled orbital shaker to enhance reaction equilibrium at room temperature of 25 ± 1 ^oC. The equilibrium concentration of phosphate desorption were determined after 24 h, centrifugation also performed before concentration analyzing.

2.3 Results and discussion

2.3.1 Characterization of Kanuma mud absorbent

The XRD spectrums are shown in Figure 2.1c. The peaks were complex in spectrum and some of them were overlapped because of the complicated components in Kanuma mud. The XRD patterns of the Kanuma mud are strong with distinct peaks, implying a higher crystallinity degree of the major components. According to the XRD data analyzing, the reflections described in the figure might be defined as boehmite (JCPDS 74-1895), goethite (JCPDS 81-0463) and periclase (JCPDS 45-0946). Table 2.1 showed the composition of Kanuma mud from an EDX analysis, it is obvious that the mainly composition of Kanuma mud are metal oxides.

The scanning electron microscope (SEM) images of Kanuma mud adsorbents are shown in Figure 2.1a and Figure 2.1b. It is obviously observed that lamellar and porous morphology widely exist. It indicated that these structures supplied larger BET surface which would play a positive effect on adsorption sites during phosphate adsorption process. The results of BET is shown in Table 2.1, indicating that Kanuma mud possessed a large specific surface area and total pore volume which largely higher than other similar materials, such as fly ash, slag and red mud (0.66, 1.11, 14.09 m^2 g^{-1}, respectively) [72]. This result implies that Kanuma mud can be used as an absorbent for phosphate adsorption. In addition, the BJH pore size distribution was illustrated in Figure 2.1d. The proportions of pore diameter in the range from 20 to 80 μm, 6 to 20 μm and over 80 μm accounted for 26.71%, 39.51% and 15.14%, respectively, indicating that Kanuma mud is a typical mesoporous (majority pores distribution: 2 - 50 nm) geomaterial according to IUPAC classification [73].

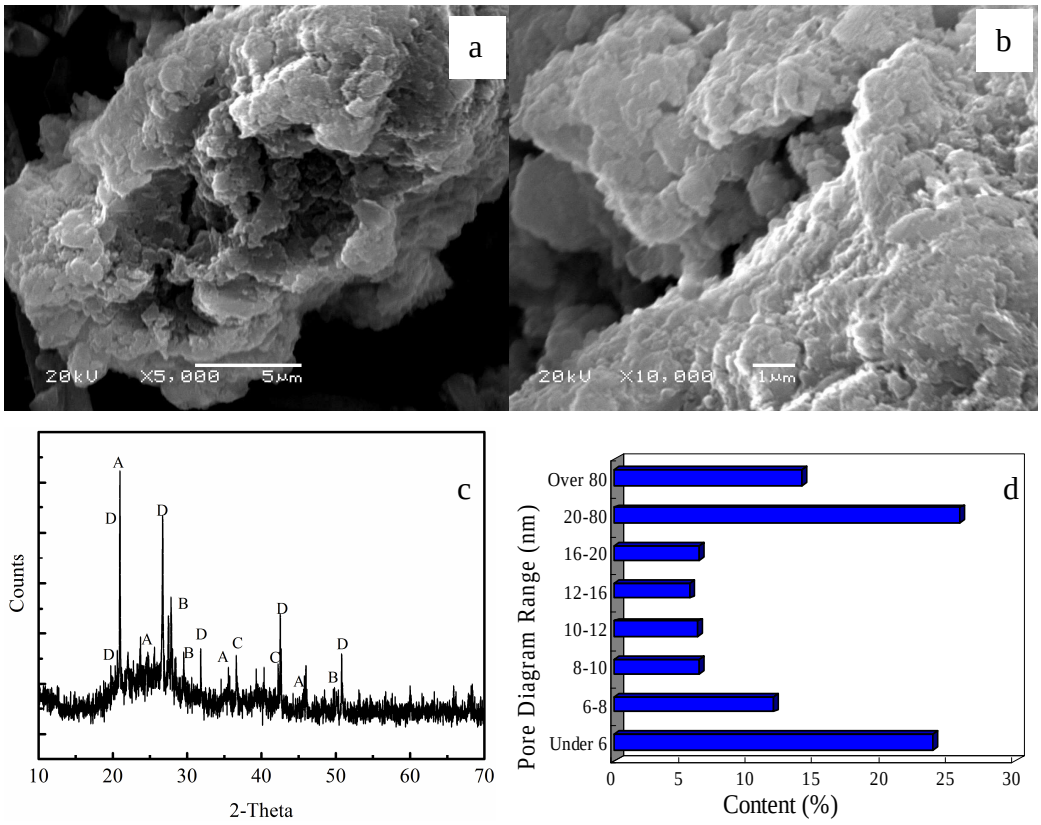

Figure 2.1. Morphology and characterization of Kanuma mud: (a) Scanning electron microscope micrographs of Kanuma mud adsorbents: 20kV, ×5000; (b) 20kV, ×10000; (c) XRD spectrums patterns of Kanuma Mud, A: boehmite; B: goethite; C: Periclase; D: Al_2O_3; (d) Adsorption BJH Pore Size Distribution.

Table 2.1 The BET data and composition of Kanuma mud.

	BET Surface area	Langmuir Surface area	Pore Volume
Values	107.04 $m^2 g^{-1}$	91.360 $m^2 g^{-1}$	0.1694 mL g^{-1}
Correlation coefficient (R^2)	0.999	0.998	

EDX analysis results

Content (%)	Fe_2O_3	MgO	Al_2O_3	SiO_2	CaO	MnO
	2.2	0.58	38.41	56.11	2.1	0.62

2.3.2 Adsorption isotherm

The equilibrium uptake capacity of phosphate q_e (mg g^{-1}) was calculated by the following equation (2.1):

$$q_e = \frac{(C_i - C_e) \times V}{1000w} \tag{2.1}$$

where C_i and C_e are the initial and equilibrium phosphate concentrations (mg L^{-1}), V is the volume of phosphate solution (mL), w is the mass of adsorbent (g), respectively.

In order to estimate the maximum phosphate adsorption capacity of Kanuma mud, Langmuir and Freundlich isotherm models were applied to describe the adsorption behavior. The Langmuir isotherm and the Freundlich isotherm can be presented by [74]:

$$\frac{1}{q_e} = \frac{1}{Q} + \frac{1}{bQ}\frac{1}{C_e} \tag{2.2}$$

$$\log q_e = \log K_f + \frac{1}{n}\log C_e \tag{2.3}$$

where q_e is equilibrium phosphate concentration on adsorbent (mg g^{-1}), C_e is equilibrium phosphate concentration in solution (mg L^{-1}), Q is estimated monolayer capacity of the adsorbent (mg g^{-1}), b is adsorption constant, K_f (mg g^{-1}) is the Freundlich constant, and n is the Freundlich exponent. While Langmuir isotherm parameters Q and b could be obtained by plotting ($1/q_e$) versus ($1/C_e$), Freundlich isotherm parameters could be obtained by plotting $\log q_e$ versus $\log C_e$. The Langmuir model is often used to demonstrate a monolayer distribution of adsorbate within the adsorbent, and the Freundlich isotherm model usually tend to describe a

heterogeneous adsorption process, and assuming that different sites with several adsorption energies were complicated [75].

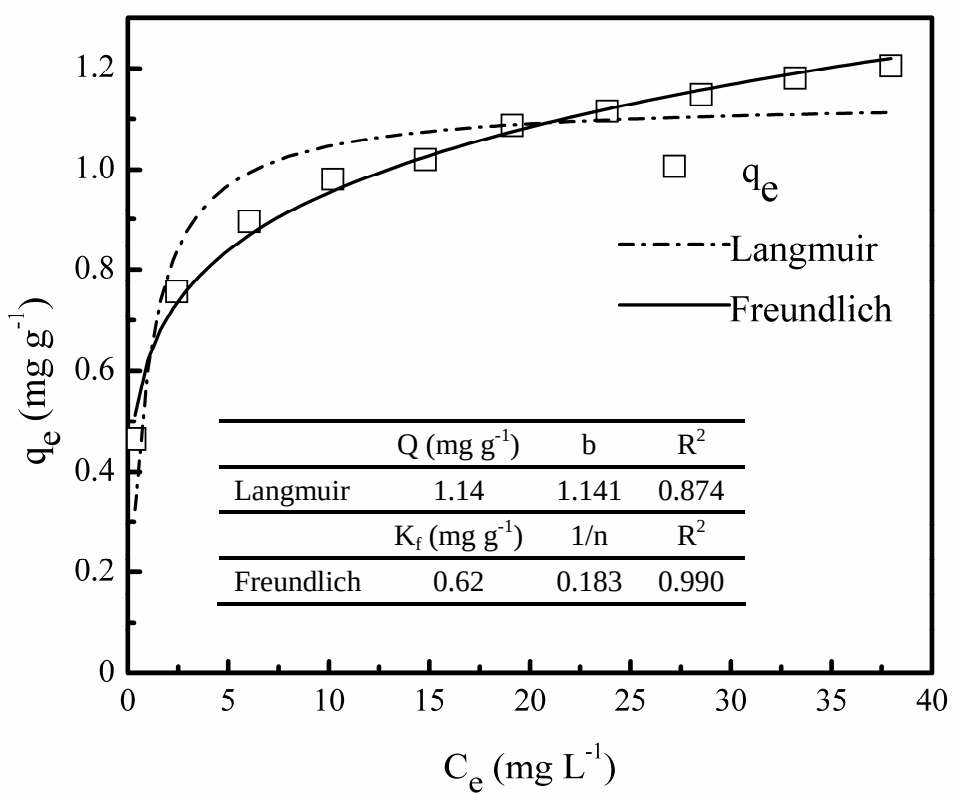

Figure 2.2. The curves and parameters of Langmuir and Freundlich isotherms. Initial P concentrations: 5 to 50 mg L^{-1}. Temperature: 25 ± 1 ^{o}C. Adsorbent dosage: 10g L^{-1}.

Figure 2.2 shows the curves and corresponding isotherm parameters of Langmuir and Freundlich isotherm models. The R^2 obtained from Eq. (2.3) was higher than 0.99, indicating a very good mathematical matching by Freundlich models. The correlation coefficient of Freundlich model (R^2 = 0.990), much greater than that of Langmuir model indicates that the phosphate adsorption onto Kanuma mud is more like a complex adsorption process with diverse energetic distribution of adsorption sites and with interaction between the adsorbate. This observation might also be contributed by the different phosphate affinities for various metal oxides existed in Kanuma mud. The estimated monolayer maximum adsorption capacity of Kanuma mud was 1.14 mg g^{-1}, the practical value would be larger due to the heterogeneous adsorption process. In this study, the practical adsorption capacity was 2.13 mg g^{-1} under the condition of lower dosage (4 g L^{-1}) and higher initial concentration (50 mg L^{-1}). This value was much larger than many adsorbents, such as furnace slag (1.43 mg g^{-1}) [74] and red mud (0.58 mg g^{-1}) [76]. Besides, the constant of K_f and n in Freundlich model denote the adsorption capacity of the adsorbent and deviation from linearity of the adsorption process, respectively. A higher value of n (n > 1) implies favorable adsorption. In this study, n is 5.46, indicating that Kanuma mud has the potential capability for phosphate adsorption from aqueous solution. In addition, the Kanuma mud can be used in agriculture and horticulture after phosphate adsorption in practice.

Table 2.2 The parameters of pseudo first-order kinetic model and pseudo second-order kinetic model for phosphate adsorption using Kanuma mud.

Initial Con.	Pseudo first-order model			Pseudo second-order model		
	q_e (mg g^{-1})	k_1 (min^{-1})	R^2	q_e (mg g^{-1})	k_2 (g(mg $min)^{-1}$)	R^2
10 mg L^{-1}	0.094	$1.87*10^{-3}$	0.955	0.47	0.203	0.999
15 mg L^{-1}	0.13	$1.88*10^{-3}$	0.929	0.58	0.166	0.999
20 mg L^{-1}	0.16	$1.85*10^{-3}$	0.936	0.71	0.131	0.999

2.3.3 Adsorption kinetics and effect of contact time.

The effects of contact time and adsorption kinetics study always play an important role in the evaluation of adsorption process and it can provide further information on the process mechanisms. In this study, pseudo first-order kinetic model and pseudo second-order kinetic model were applied to examine the kinetics of phosphate adsorption onto Kanuma mud.

The pseudo first-order kinetic model is expressed as Eq. (2.4) and can be simplified as Eq.(2.5) after integration with the boundary conditions being set ($q_t = 0$ and q_t when t = 0 and t, respectively) [77]:

$$\frac{dq_t}{dt} = k_1(q_e - q_t) \tag{2.4}$$

$$\log(q_e - q_t) = \log q_e - k_1 t \tag{2.5}$$

where q_e (mg g^{-1}) and q_t (mg g^{-1}) are phosphate adsorbed amount at equilibrium and time t, respectively; k_1 is the rate constant for the pseudo first-order kinetic model (min^{-1}).

The pseudo second-order kinetic model is expressed as Eq. (2.6), which can be simplified as Eq. (2.7):

$$\frac{dq_t}{dt} = k_2(q_e - q_t)^2 \tag{2.6}$$

$$\frac{t}{q_t} = \frac{1}{k_2 q_e^2} + \frac{t}{q_e} \tag{2.7}$$

where k_2 is the rate constant for pseudo second-order kinetic model (g (mg min) $^{-1}$). The values of k_2 and q_e are calculated from a plot of (t/q_t) versus t.

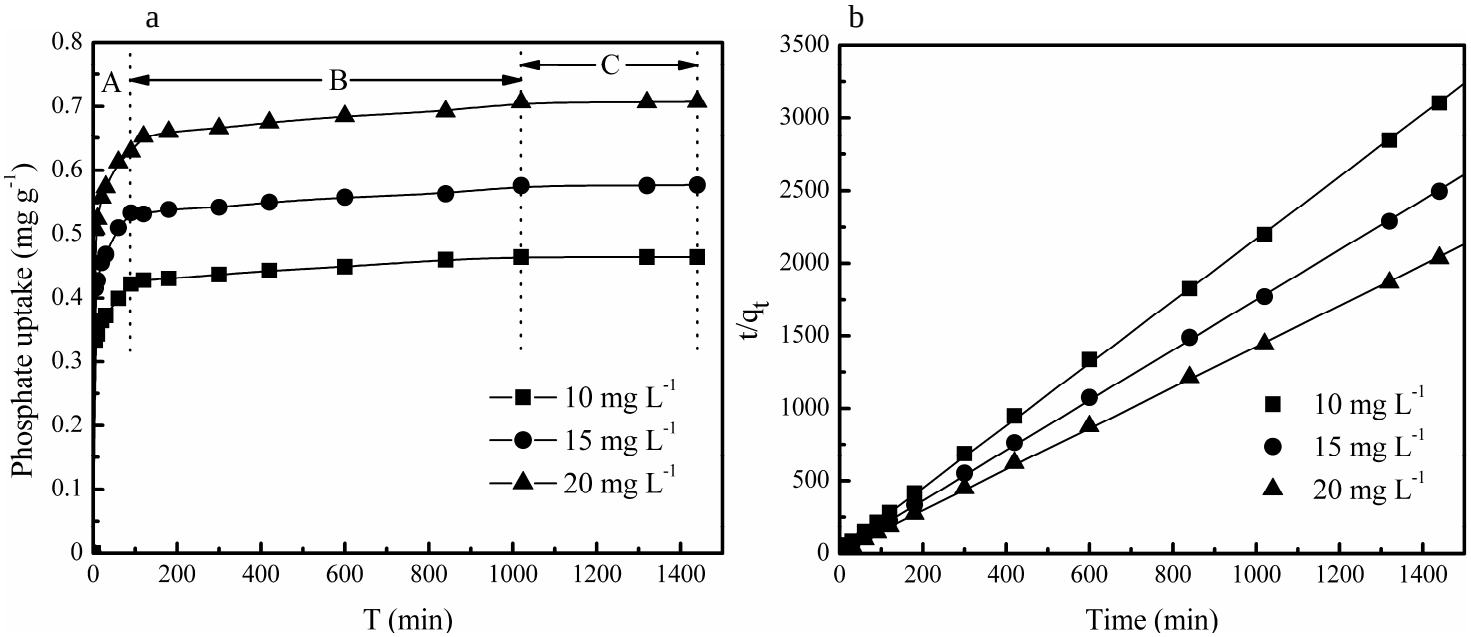

Figure 2.3. The effect of contact time and curves of pseudo second-order kinetic model: (a) The effect of contact time with different initial concentration of phosphate; (b) The curves of pseudo second-order kinetic model with different initial concentration of phosphate. Initial P concentration: 10, 15 and 20 mg L^{-1}. Temperature: 25 ± 1 ^{o}C. Dosage: 20 g L^{-1}.

Figure 2.3a shows the effect of contact time on phosphate adsorption using Kanuma mud, and a three-step natural process was exhibited: a rapid reaction step (step A) in 0 - 90 min; a slow reaction step (step B) in 90 - 1020 min and an equilibrium step after 1020 min (step C). About 90.9, 90.8 and 88.9 % (when initial concentration was 10, 15 and 20 mg L^{-1}, respectively.) of whole adsorption process was completed in step A. The phosphate was rapidly adsorbed until 90 min maybe attributed to with the surface adsorption, and more quantities of available vacant adsorption sites supplied advantageous effects in step A. In addition, a higher driving force [60] caused by high concentration enhance the contact chance between the adsorbate and absorbent hence a higher adsorption efficiency on phosphate by Kanuma mud. Further, the step B lasted about 17 h until the phosphate adsorption to equilibrium. During this stage, a little amount of phosphate was absorbed mainly due to the quantities decrease of vacant adsorption sites on the surface of Kanuma mud, and the decrease of the driving forces due to the decrease of phosphate concentration in solution. The equilibrium was achieved at 1020 min, no advance removal efficiency reflected in equilibrium step (Step C). Step B maybe related with the inner diffusion adsorption of the Kanuma mud and to the possibility of chemical precipitation reaction with the metal components contained in Kanuma mud, such as Fe, Al, Ca, Si, etc [52, 67, 78, 79].

The fitted curve and parameters of kinetic models are shown in Figure 2.3b and Table 2.2 It is clear that the phosphate adsorption process onto Kanuma mud could be

well described by pseudo second-order model because of the higher correlation coefficient ($R^2 > 0.999$).

2.3.4 Effect of pH on phosphate adsorption

Phosphate dissociation equilibrium in aqueous solution is pH-dependent, which can be presented in Figure 2.4a [55]:

For a detailed description, with pHs ranges from 5 to 10, $H_2PO_4^-$ and HPO_4^{2-} are majority species. To be more clear, $H_2PO_4^-$ prevails when pH ranges from 5 to 7 and the content of HPO_4^{2-} is higher when pH ranges from 7 to 10; with pHs ranges from 10 to 12, HPO_4^{2-} prevails than PO_4^{3-}, and PO_4^{3-} becomes majority when pH is higher than 12.

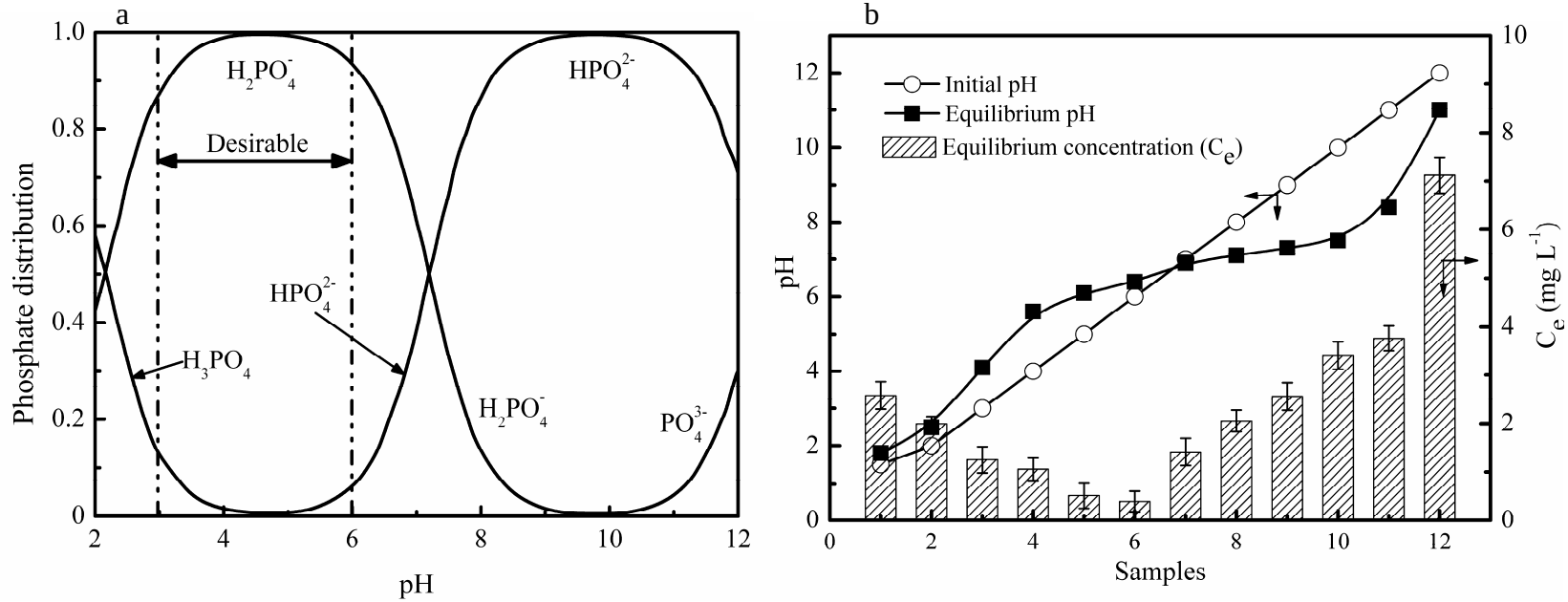

Figure 2.4. Phosphate distribution and effect of pH on phosphate adsorption: (a) Phosphate distribution in different pH solution [80]; (b) Effect of pH change on phosphate adsorption (The arrows on the curve and bar show the corresponding axis of data).

It is well known that phosphate is usually considered to be removed through an inner-sphere ligand ion exchange mechanism [81]. The metal oxidation hydrolyze reaction can supply OH^- which is possibly used in inner-sphere ligand ion exchange mechanism [82]:

$$M_xO_y + yH_2O \rightarrow xM^{(2y/x)+} + 2yOH^- \tag{2.8}$$

The produced $M^{(2y/x)+}$ in metal oxidation hydrolyze would uptake phosphate through an electrostatic interaction which could be expressed by Eq. (2.9)

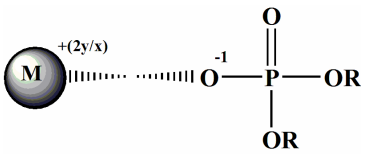

(2.9)

Considering the hydroxyl protonation and the different phosphate species dominated in different pH solutions, the following reactions may be included in phosphate removal through Kanuma mud:

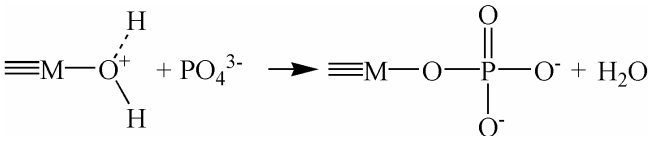

(2.10)

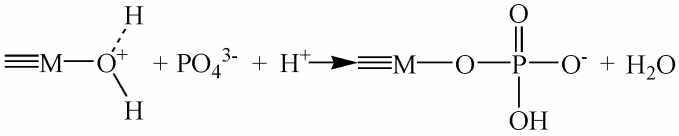

(2.11)

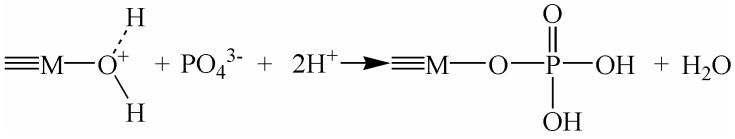

(2.12)

The overall reaction could be expressed as:

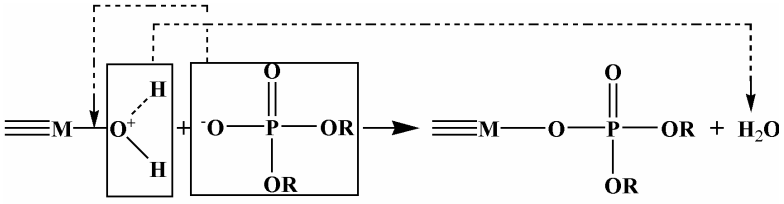

(2.13)

In the case of phosphate at different pH condition, the binding sites are protonated ($M\text{-}OH_2^+$), Consequently, a higher coulombic attraction forces between the binding sites and phosphate in addition to chemical interaction leads to higher phosphate uptakes, which are shown in Eqs. (2.10) to (2.13).

Further, phosphate-metal precipitation reaction seems to be an alternative explanation, which could be presented as:

$$xPO_4^{3-} + 3M^{x+} = M_3(PO_4)_x \quad (2.14)$$

where M is metal component, such as Al, Fe, Ca, Si, etc.

The phosphate adsorption by Kanuma mud can be profoundly affected while changing of pH value. The equilibrium phosphate removal efficiency slightly varied between 87.52 - 96.06 % when solution pH ranges from 3.0 to 6.0. The results (Figure 2. 4b) showed that the removal efficiency of phosphate was founded at pH value of 6 when Kanuma mud was used as absorbent. Figure. 2.4a and Eqs. (2.10) - (2.12) indicatd that monovalent dihydrogen phosphate ($H_2PO_4^-$) and divalent hydrogen phosphate (HPO_4^{2-}) could be well adsorbed by Kanuma mud. The phosphate uptake decreased sharply with the increasing of pH value, especially at pH of 12 (0.144 mg g^{-1}). This observation was possibly caused by the deprotonation of oxide/hydroxides under higher pH conditions which could be expressed as:

$$\equiv M - OH \rightarrow \equiv M - O^- + H^+ \quad (2.15)$$

This reaction may result in a negative change of surface charge of Kanuma mud and hence the decrease of phosphate adsorption capacity. In addition, the functional group (-OH) were destroyed in the deprotonation process, leading to phosphate

release and decrease in phosphate adsorption due to electrostatic repulsion. Also, the competitive adsorption of OH^- ions probably plays a significant role within high pH conditions.

On the other hand, the phosphate uptake also decreased slowly with the decreasing of pH value in solution, which reduced to 74.27% at pH 1.5. As mentioned above, $H_2PO_4^-$ could be removed effectively by Kanuma mud (Eq. (2.12)), thus H_3PO_4 seems difficult to be adsorbed (Figure 2.4a).

Kanuma mud was found rich in Fe and Al contents (Table 2.1). These metal oxides and hydroxides are mainly existed as oxygen atoms and hydroxyl groups form on the surface, providing the absorbing sites for phosphate adsorption. The charges of metal oxides and hydroxides complexes in the materials are easily affected by solution pH, which also affects the phosphate adsorption. When pH value decreased, the metal oxides/hydroxides became unstable and started to dissolve, leading to the number decrease of adsorption sites for phosphate adsorption. The result is similar with that of M. Özacar [83] who claimed that maximum phosphate adsorption occurred at pH 5 using alunite, and also agrees with results of Xiong and Mahmood [67] who obtained the maximum phosphate adsorption at pH 6.5 and the adsorption amount decreased with either decreasing or increasing pH when using peat as a phosphate absorbent.

2.3.5 Effect of temperature on phosphate adsorption

The effect of temperature on phosphate adsorption was investigated, and the results are shown in Figure 2.5a. The results showed that the phosphate adsorption from aqueous solution almost unchanged when initial concentration was comparatively low, but the phosphate uptake decreased with the increase of temperature when initial concentration of phosphate was higher than 5 mg L^{-1}. The removal efficiency of 57.44% at 35 °C and increased to 61.84% at 25°C, 64.48% at 5 °C, respectively. It is a rare (most of mineral absorbents was endothermic process.) in agreement with the reports on phosphate adsorption by peat [67] and fly ash [84]. It is obvious that the process of phosphate adsorption was an exothermic process of which decreasing of temperature enhances the phosphate uptake. In practical condition, the temperature of surface water, such as lake water is always lower than 26 °C even in summer [85]. Kanuma mud could be utilized in low temperature and better removal efficiency would be achieved.

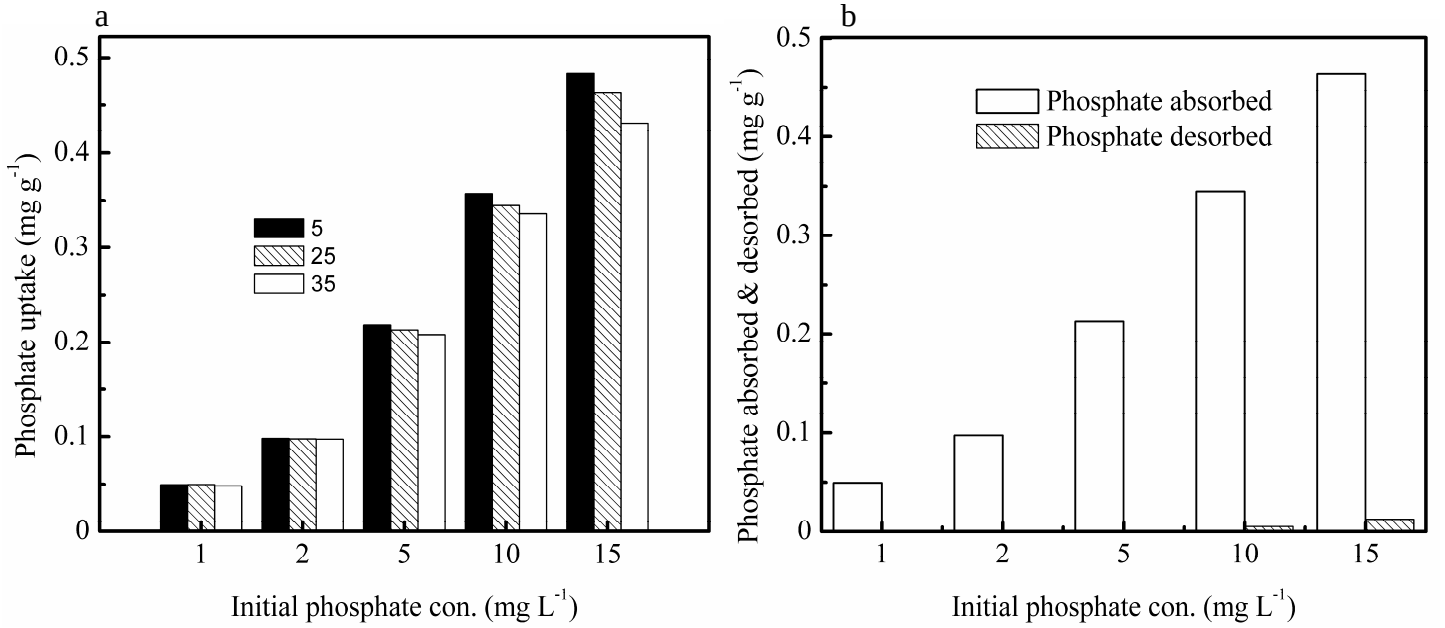

Figure 2.5. Effect of temperature and results of phosphate desorption rate: (a) Results of temperature for phosphate adsorption on Kanuma mud; Initial P concentration: 10 mg L^{-1}. Dosage: 20 g L^{-1}. Temperature: 5, 25 and 35 °C. (b) results of phosphate desorption rate from phosphate adsorbed Kanuma mud. Initial P concentration: 1, 2, 5, 10 and 15 mg L^{-1}. Temperature: 25 ± 1 ^{o}C.

2.3.6 Desorption study

The phosphate desorption experiments were performed with 5 initial phosphate concentrations (1, 2, 5, 10 and 15 mg L^{-1}) at pH value of 6 and room temperature. The adsorption capacity was calculated as 0.05, 0.11, 0.22, 0.35 and 0.46 mg g^{-1} with initial concentration of 1, 2, 5, 10 and 15 mg L^{-1}, respectively.

Figure 2.5b shows that almost no desorption occurred after phosphate adsorption onto Kanuma mud when phosphate adsorbed was lower than 0.11 mg g^{-1} at a dosage of 20 g L^{-1}. With the increase of phosphate adsorbed on adsorbent, a little amount of adsorbed phosphate started to be desorbed. The result showed that 0.012 mg g^{-1} of adsorbed phosphate could be desorbed when initial P concentration is 15 mg L^{-1}. Therefore, phosphate absorbed Kanuma mud may be suitable for applying as a soil fertilizer due to the slow release rate of absorbed phosphate. Thus, no further treatment was required for the phosphate adsorbed Kanuma mud.

2.4 Conclusions

According to this study, the Kanuma mud exhibited desirable phosphate adsorption ability. The adsorption process consisted of three steps: rapid, slow and a stable process. The former finished in 110 min and the latter extended to 24 h even more. The Freundlich isotherm model and pseudo-second-order model can well describe the sorption process. The phosphate adsorption efficiency mainly depended on pH and temperature, in which the optimal adsorption amount was the best at pH 6 and comparatively low temperature can enhance the adsorption efficiency. The

phosphate sorption capacity was also related to the metal oxide component exist in Kanuma mud. A little amount of phosphate on the absorbent was desorbed. Besides, the Kanuma mud which adsorbed phosphate is friendly to the environment. No further treatment is required for phosphate absorbed Kanuma mud, and the absorbed absorbent can be used as soil fertilization.

Chapter 3 A novel tablet porous material developed as adsorbent for phosphate removal and recycling

3.1 Introduction

A large amount of phosphate discharged from untreated wastewaters, fertilizer industries, etc. into water body is often responsible for algal bloom and eutrophication [86-88], especially in lakes, reservoirs and coastal areas. On the other hand, P element is necessary for human beings, and the lack of P will limit food production for our growing world population [89]. Besides, phosphate can also be used in other areas, such as photocatalysis [90], electrochemistry [91] and bioceramics [92]. Phosphorus as an un-renewable resource is estimated to be depleted in 50 - 100 years based on current global reserves [93]. So P recycling from wastewater and reusing is important and urgent.

Adsorption may be the most promising process when taking P removal efficiency, operation convenience, P recycling and reusing into consideration. Diverse adsorbents were tested for phosphate removal, such as peat [67], palygorskite [53], alunite [52], mussel shells [57], active red mud [94], ferric sludge [95], dolomite [21], and resin [47]. Although effective phosphate removals have been achieved, these adsorbents can’t be widely applied in practice due to their difficulties in separation from aqueous phase (powder materials, such as bentonite and red mud, etc) or high cost (resin). Thus some new, effective and low-cost adsorbents are still necessary to be developed to solve the above mentioned problems.

In Chapter 2, Kanuma mud was used for phosphate removal and exhibited effective phosphate removal efficiency. The composition of K-mud mainly consists of silicon and metal oxides, such as SiO_2, Al_2O_3, Fe_2O_3, MgO, CaO, etc [70].

Further, in this chapter, a tablet porous material (TPM) was developed from K-mud, corn starch and calcium oxide to remove phosphate. Its physical, chemical and surface characteristics, isotherms model, and kinetic model were investigated. In addition, some influencing factors (such as dosage, pH and temperature) and TPM regeneration are also discussed.

3.2 Materials and methods

3.2.1 Synthesis of tablet porous material.

K-mud (bought from the Makino Store, Kiyosu, Japan) was manually smashed and sieved, and the particles less than 300 μm were selected and used in this study. Corn starch and CaO (analytical reagent) were supplied by Wako Pure Chemical industries Ltd, Japan.

The TPM was synthesized as the following process (Figure 3.1), and the developed TPM were cooled to room temperature and used in the following experiments.

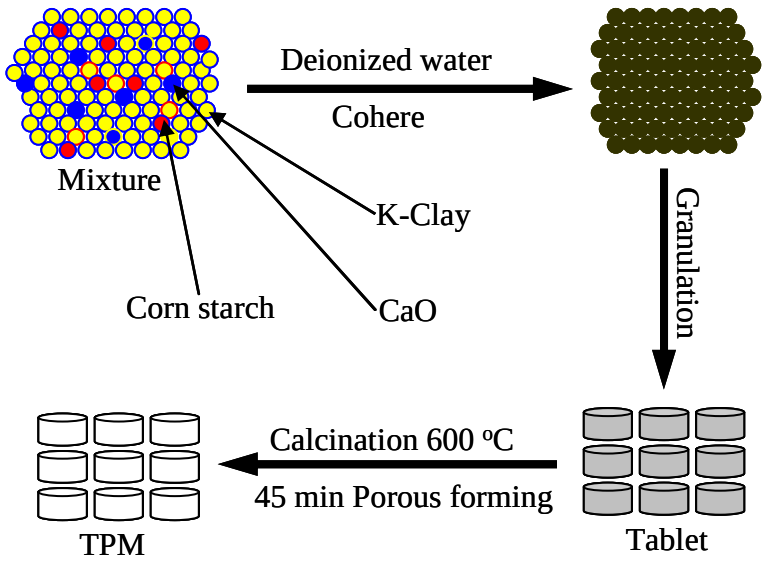

Figure 3.1. The procedure of TPM synthesis. Mass ratio of K-mud: corn starch: CaO is 4: 0.5: 1.

3.2.2 Phosphate adsorption experiments

A stock solution of 50 mg L^{-1} phosphate was prepared by dissolving KH_2PO_4 (anhydrous, analytical grade) in deionized water. All the adsorption experiments were conducted more than triplicate in 50 mL test tubes in a thermostat (except the thermodynamics experiments). Considering practical condition, all experiments were performed without shaking.

3.2.2.1 Isotherms experiment

A number of 0.2 g TPMs were added into test tubes respectively under initial phosphate concentration ranged from 5 to 50 mg L^{-1} and initial pH 7.0. Then the test tubes were set in the thermostat (25 ± 1 ^{o}C).

3.2.2.2 Kinetic experiment

One gram TPM was individually dosed into test tubes containing 50 mL of 10 mg L^{-1} phosphate solution. The sampling time intervals were 5, 10, 20, 30, 90, 120 and 180 min, respectively (initial pH 7.0, 25 ± 1 ^{o}C).

3.2.2.3 Effect of pH

Fifty milliliter phosphate solutions (10 mg L^{-1}) were added respectively in 11 test tubes with 1 g TPM dosed. 0.1 M HCl or NaOH were used to adjust the initial solution pH ranged from 2.0 to 12.0. All the test tubes were capped to avoid evaporation and the pH values were determined after 2 h (25 ± 1 ^{o}C).

3.2.2.4 Thermodynamics and effect of temperature

The thermodynamics and influence of temperature on phosphate adsorption onto TPM was carried out at temperatures ranging from 288.15 to 308.15K with an initial

phosphate concentration between 5 and 20 mg L^{-1} (initial pH 7.0, a fixed TPM dose of 4 g L^{-1}).

3.2.2.5 Effect of dosage

Twenty mg L^{-1} of phosphate solution was used for adsorption under different TPM dosage (initial pH 7.0, 25 ± 1 ^{o}C). The TPM dosage varied from 5 to 50 g L^{-1}.

3.2.3 TPM regeneration and phosphate recycling test

In this trial 50 mg L^{-1} of phosphate solution was used for TPM adsorption. After adsorption, the TPMs were collected and used for phosphate desorption. HCl (0.2 mol L^{-1} and 0.5 mol L^{-1}) and NaOH (0.1 mol L^{-1}) were utilized to test the possibility of phosphate recycling and TPM regeneration.

3.2.4 Analytical methods

TPM was characterized by Energy Dispersive X-Ray Spectroscopy and scanning electron microscope (SEM XL40 series philips, holland) to obtain its physical, chemical and surface characteristics; Brunauer-Emmett-Teller (BET) specific surface area was obtained by a analysis device (Coulter SA3100, US) using the He-N_2 method. All the equilibrium phosphate concentration was analyzed with the ascorbic acid method (4500-P E) [71].

3.3 Results and discussion

3.3.1 Characterization of TPM

Figure 3.2a is the photo of pristine TPM (Φ7mm, H2mm); the SEM images of TPM adsorbents (before and after phosphate adsorption) are illustrated in Figure 3.2b and Figure 3.2c. The images obviously showed that porous texture and structure were widely developed at the surface of TPM; it might be molded during the incineration process in which corn starch would be burned off leaving porous structure in TPM. The result indicated TPM would naturally develop a comparatively larger specific surface area that plays a positive effect on adsorption sites during phosphate adsorption onto TPM. Furthermore, the surface feature of TPM after phosphate adsorption was different with raw TPM to a certain degree, assuming that metal-hydroxyl-phosphate ligand component [96] and phosphate-metal chemical precipitation [97] might bring about these morphological changes of TPM surface during phosphate adsorption.

The EDX result is shown in Figure 3.2d, and the detailed composition of TPM is summarized in Table 3.1.

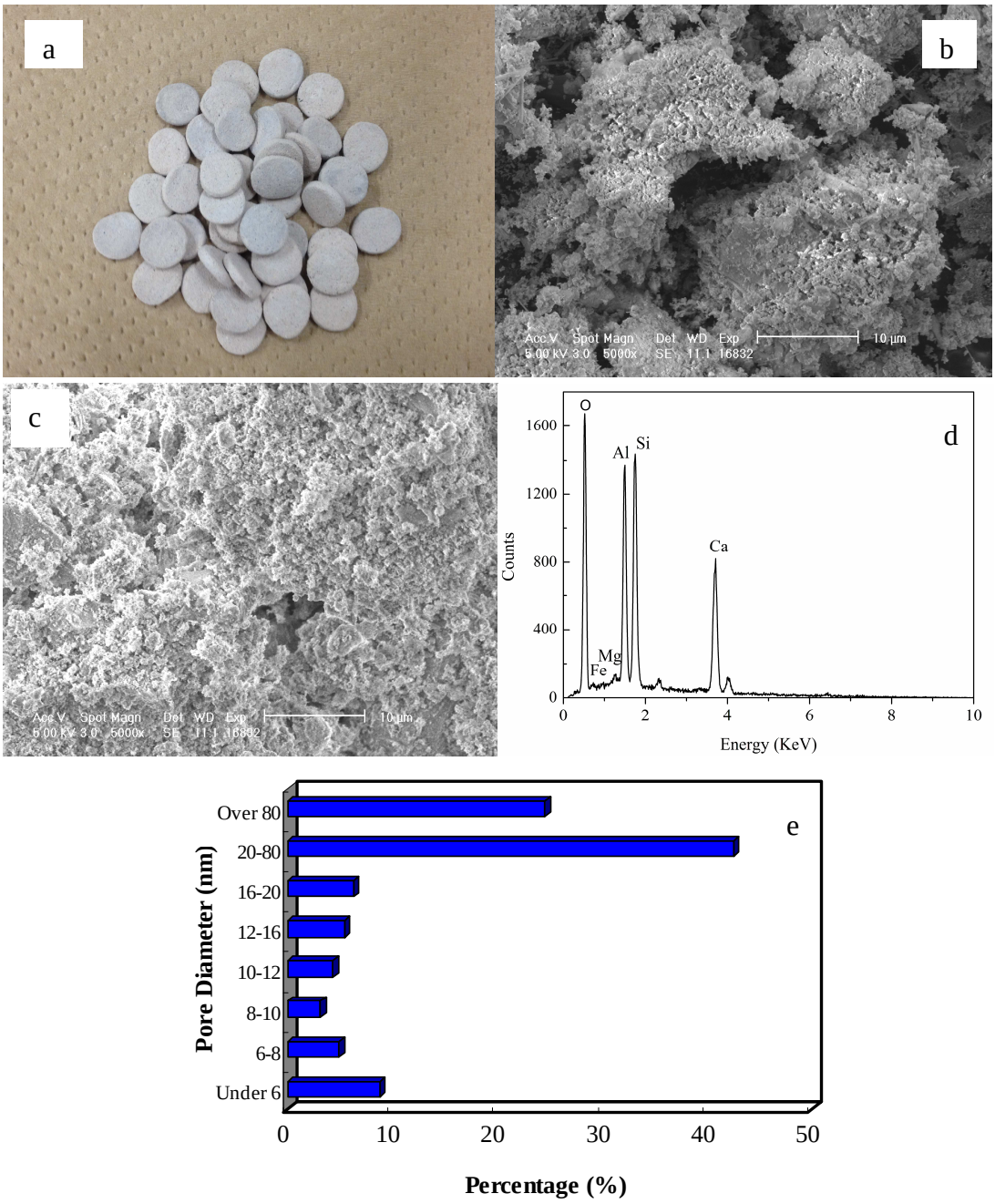

Figure 3.2. TPM characterization: (a) photo of pristine TPM; (b) SEM image of TPM before phosphate adsorption, 5000x; (c) SEM image of TPM after phosphate adsorption, 5000x; (d) EDX results of TPM; (e) pore diameter distribution of TPM.

Clearly, TPM is mainly composed of silicon and metal oxides such as Al_2O_3, SiO_2 and CaO. Al_2O_3 was reported as a good adsorbent for phosphate by surface precipitation [98], and the added CaO in TPM could be transformed into calcium hydroxides in aqueous solution and supplied large amount of functional groups (Ca^{2+}, OH^-) to enhance the chemical precipitation and inner-sphere ligand exchange process.

The result of specific surface area of TPM and K-mud (Table 3.1) showed that BET surface area was 107.04 m^2 g^{-1} for raw K-mud and decreased to 15.401 m^2 g^{-1} for TPM, due to the fact that the particle size of raw K-mud lower than 300 μm while the diameter of TPM was about 7 mm. The specific surface area of TPM was similar with red mud, 14.09 m^2 g^{-1} [94] but lower than hydrotalcite, 44 m^2 g^{-1} [60]. In addition, the pore size distribution (Figure 3.2e) indicated that TPM was a typical mesoporous material according to IUPAC classification [73]. The proportion of pore diameter in the range from 20 to 80 μm, 6 to 20 μm and over 80 μm accounted for 42.51%, 24.18% and 24.54%, respectively. Actually, the higher mass ratio of corn starch used as a pore-enhancer could increase the pore volume of TPM, but the structure stability of TPM would decrease with the increase of mass ratio of corn starch. In this study, the 9.09% (0.5/5.5) mass ratio of pore-enhancer was desirable in TPM synthesis process.

Table 3.1 The detailed results of EDX and specific surface area of K-mud and TPM.

Sample	BET surface area			Total pore Volume
	Values (m^2 g^{-1})	Monolayer volume (mL g^{-1})	Correlation coefficient	Values (mL g^{-1})
K- mud	107.0	24.6	0.999	0.169
TPM	15.4	4.11	0.998	0.085

EDX analysis results (TPM)

Content (%)	Fe_2O_3	MgO	Al_2O_3	SiO_2	CaO
	14.7	9.1	24.5	29.8	21.9

3.3.2 Phosphate adsorption isotherms and performance of TPM

The equilibrium uptake capacity of phosphate, q_e (mg g^{-1}), was calculated by Eq. (2.1).

In order to examine the maximum phosphate adsorption capacity of TPM, Langmuir and Freundlich isotherm models were applied to fit the experimental data, which can be described as Eq. (2.2) and Eq. (2.3), respectively.

The Langmuir model is often used to demonstrate a monolayer distribution of adsorbate within the adsorbent, and the Freundlich isotherm model usually tend to describe a heterogeneous adsorption process assuming that different sites with several adsorption energies were complex [75].

The corresponding isotherms constants of Langmuir and Freundlich models for phosphate adsorption on TPM were summarized in Table 3.2 and Figure 3.3d. The R^2 obtained from Eq. (2.2) and Eq. (2.3) were both higher than 0.98, indicating a very good mathematical fit by both models. And the correlation coefficient of Freundlich model (R^2 = 0.990) greater than that of Langmuir model indicated that the phosphate adsorption through TPM is more like a multilayer adsorption process with diverse energetic distribution of adsorption sites and with interaction between adsorbed mass. This observation might also be contributed by the different phosphate affinities for various metal oxides existed in TPM. The estimated maximum adsorption capacity (q_{max}) obtained from Langmuir model is 4.39 mg g^{-1}, which is close to the experimental maximum adsorption capacity, 4.01 mg g^{-1} when initial phosphate concentration is 80 mg L^{-1} (TPM dosage: 4 g L^{-1}).

Table 3.2 The parameters of kinetics and isotherm models.

Kinetics models					
Pseudo first-order model			Pseudo second-order model		
q_e (mg g^{-1})	k_1 (min^{-1})	R^2	q_e (mg g^{-1})	k_2 (g (mg min) $^{-1}$)	R^2
0.13	0.016	0.929	0.50	0.606	0.999

Isotherm models					
Langmuir model			Freundlich model		
q_{max} (mg g^{-1})	b (L mg^{-1})	R^2	K_f (mg g^{-1})	n	R^2
4.39	0.243	0.986	1.66	3.89	0.990

Table 3.3 Comparison of maximum phosphate adsorption capability of TPM with other mineral adsorbents.

Adsorbent	q_{max} (mg g^{-1})	Source
Na-natural zeolite	2.19	[72]
Natural palygorskite	3.73	[53]
Bentonite	5.54	[99]
Red mud	0.58	[76]
TPM	4.39	This study

Besides, The K_f of Freundlich model refers to the adsorption capacity of the adsorbent ($q_e = K_f$, when $C_e = 1$ mg g^{-1}) and is always related with temperature and the physical/chemical characteristics of adsorbents. The n of Freundlich model denotes the deviation from linearity of the adsorption, such as heterogeneity factor. It also indicates the intensity change of the adsorption process. A higher value of n (n > 1) indicates favorable adsorption. It was also found that the newly developed TPM was superior to other natural clay mineral (mud) adsorbents based on their maximum phosphate adsorption capacities (Table 3.3), implying that TPM had the potential for phosphate removal from wastewater in practice.

3.3.3 Kinetics and effect of contact time

The effect of contact time and kinetics study is important to evaluate adsorption process and it can provide further information on the process mechanisms. In this study, pseudo first-order model and pseudo second-order model were applied to examine the kinetics of phosphate adsorption onto TPM.

The pseudo first-order model is expressed as Eq. (2.4) [77] and can be simplified as Eq. (2.5) after integration with the boundary conditions being set($q_t = 0$ and q_t when t = 0 and t, respectively). The pseudo second-order model is expressed as Eq. (2.6), which can be simplified as Eq. (2.7).

The effect of contact time on TPM adsorption was shown in Figure 3.3a. Obviously, the phosphate removal process could be divided into two steps at the time of 30 min. This observation is similar with the report by Fox et al [100] who did the

experiments using river sediment, but much faster than other materials like modified bentonites [99]. 89.08% of removal efficiency was achieved at the first step (during the beginning 30 min). In this step, phosphate seemed to be removed through surface adsorption [67], and the more available vacant adsorption sites added advantageous effects to this removal process [60]. The second step started from 30^{th} min to the equilibrium, about 120 min. Only a small amount of phosphate was removed in the second step possibly due to the decrease of vacant adsorption sites on the surface of TPM.

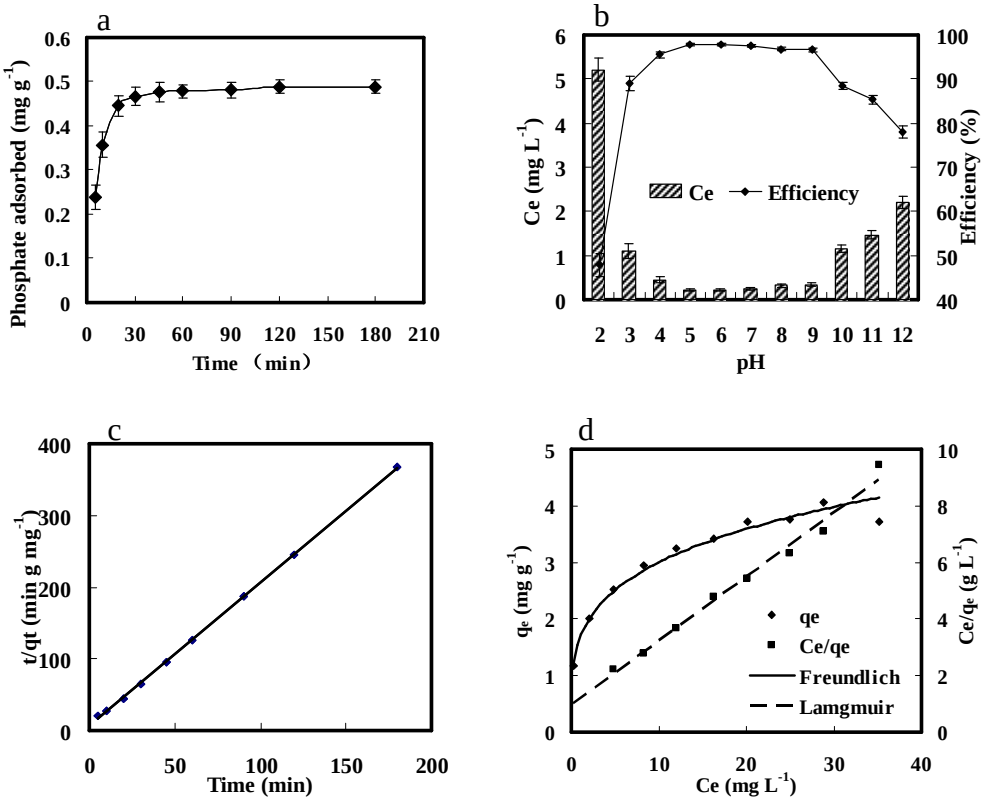

Figure 3.3. The results of phosphate adsorption experiments: (a) effect of contact time; (b) effect of pH; (c) calculation of pseudo second-order model; (d) calculation of Langmuir and Freundlich isotherm model.

The constants of pseudo first-order model and pseudo second-order model are given in Table 3.2. Based on the correlation coefficients obtained, it is clearly that the phosphate adsorption process onto TPM could be well described by pseudo second-order model under the experimental conditions (Figure 3.3c).

3.3.4 Phosphate removal mechanisms and effect of pH

Metals mainly exist as oxides and hydroxides in TPM (Table 3.1), which could provide adsorption sites for phosphate. Phosphate is usually considered to be removed through an inner-sphere ligand exchange mechanism [81]. Considering that different phosphate species dominated in different pH solutions, the following reactions may be included in phosphate removal through TPM adsorption:

(1) Surface hydroxyl deprotonation and protonation [79]:

$$\equiv M-OH \rightarrow \equiv M-O^- + H^+ \quad (3.1)$$

$$\equiv M-OH + H^+ \rightarrow \equiv M-OH_2^+ \quad (3.2)$$

(2) Phosphate-hydroxyl monodentate and protonation of adsorbed phosphate:

$$\equiv M-OH + HPO_4^{2-} \rightarrow \equiv M-PO_4^{2-} + H_2O \quad (3.3)$$

$$\equiv M-OH + H_2PO_4^- + H^+ \rightarrow \equiv M-PO_4^{2-} - 2H^+ + H_2O \quad (3.4)$$

$$\equiv M-OH + PO_4^{3-} + H^+ \rightarrow \equiv M-PO_4^{3-} - OH_2^+ \quad (3.5)$$

where M is metal component, such as Al, Fe, Ca, etc.

Meanwhile, phosphate dissociation equilibrium in aqueous solution is pH-depended, which can be presented as [54]:

$$H_3PO_4 \leftrightarrow H_2PO_4^- + H^+ \quad pK_1 = 2.16 \ (pH \leq 5.0); \quad (3.6)$$

$$H_2PO_4^- \leftrightarrow HPO_4^{2-} + H^+ \quad pK_2 = 7.20 \ (5.0 < pH \leq 10.0); \quad (3.7)$$

$$HPO_4^{2-} \leftrightarrow PO_4^{3-} + H^+ \qquad pK_3 = 10.3 \text{ (pH > 10.0)} \tag{3.8}$$

The ligand ion exchange process may influence the pH value of adsorbent-liquid system [101]; on the other hand, protonation and deprotonation reactions are easily affected by pH change. Figure 3.3b shows the results of phosphate removal by TPM adsorption under different initial solution pHs.

Restated, pH plays a significant effect on phosphate removal through TPM adsorption. The equilibrium phosphate removal efficiency almost remained unchanged (slightly varied within 96.59 - 97.79%) within solution pH range from 5.0 to 9.0. Eq. (3.7) shows that the dominant phosphate species should be monovalent dihydrogen phosphate ($H_2PO_4^-$) and divalent hydrogen phosphate (HPO_4^{2-}) when pH varied from 5.0 to 9.0, indicating that these two types of phosphate could be well adsorbed by TPM (Eq. (3.3) and (3.4)). The optimum pH value for phosphate removal was around pH 6.0. This result was in accordance with those of M. Özacar [83] and Yan et al [99] who used alunite and Fe-Al modified bentonite as phosphate absorbent, respectively. It is known that extreme pH conditions are scarcely encountered in natural surface water bodies or wastewater treatment plants, thus TPM could be used in practice without pH adjusting.

The phosphate removal efficiency decreased with further increase in solution pH and sharply decreased when pH > 10.0. At pH 12.0, the removal efficiency reduced to 78.06%, possibly caused by the deprotonation of oxide/hydroxides under higher pH conditions (Eq.(3.1)). This process may resulted in a negative change of surface charge of TPM and hence the decrease of phosphate removal efficiency. In addition,

the functional group (-OH) may be destroyed in the deprotonation process, leading to phosphate release and decrease in phosphate adsorption because of electrostatic repulsion. Furthermore, the competitive adsorption of OH^- ions probably plays an important role under high pH conditions.

On the other hand, phosphate removal efficiency exhibited a decrease trend with the decrease in solution pH when pH ≤ 3.0 (Figure 3.3b), which reduced to 47.89% at pH 2.0. Eq. (3.6) showed that the dominant phosphate species in the solution were $H_2PO_4^-$ and H_3PO_4 when pH was lower than 3.5. As mentioned above, $H_2PO_4^-$ could be removed effectively by TPM (Eq. (3.4)), thus H_3PO_4 seems unable to be adsorbed onto TPM surface. Further, under extremely low pH conditions, metal oxides/hydroxides might become unstable and started to dissolve because of large amount of H^+ coexisted in the solution, resulting in the decrease of adsorption sites for phosphate adsorption.

3.3.5 Effect of temperature and thermodynamics

The influence of temperature on phosphate removal by TPM adsorption was conducted at 288.15 K, 298.15 K and 308.15 K, respectively. The result (Figure 3.4a, initial phosphate concentration 20 mg L^{-1}) showed that phosphate removal increased with the increasing of temperature when TPM used as adsorbent. It strongly proved that phosphate removal process by TPM adsorption was an endothermic in nature, implying that the rising in temperature would enhance the binding tendency of phosphate onto the interface between TPM and phosphate [102].

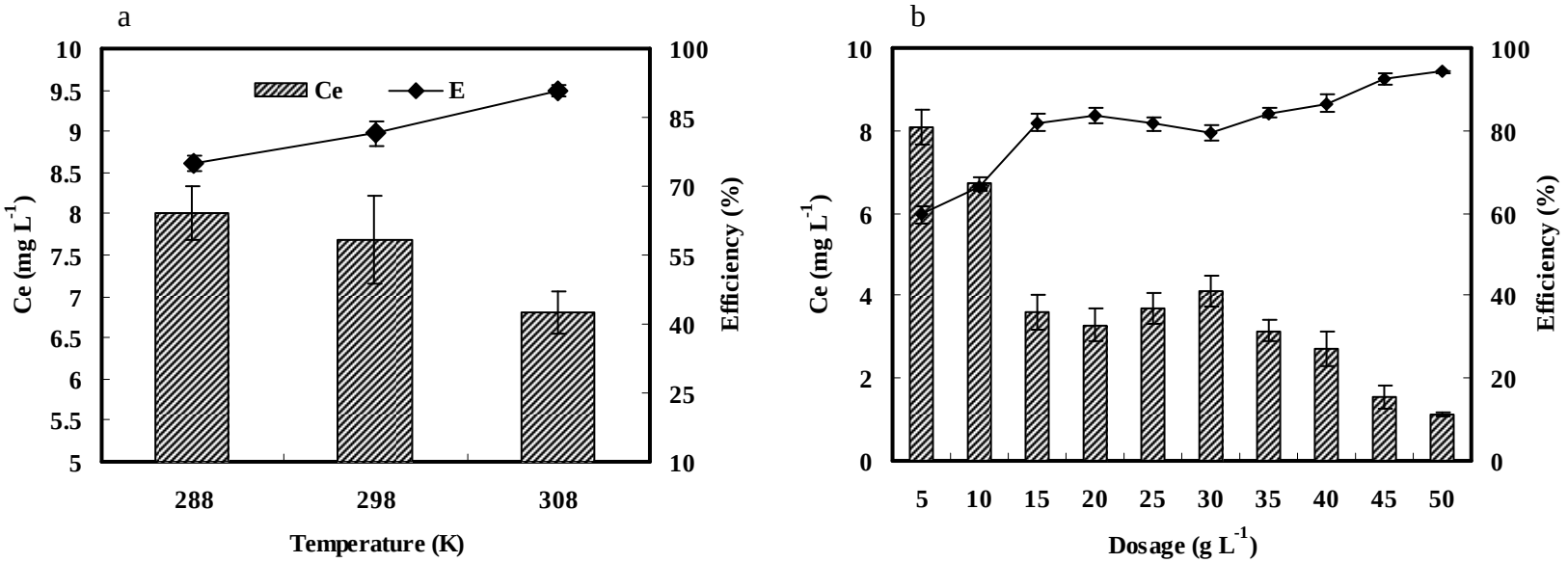

Figure 3.4. Effect of temperature and dosage: (a) effect of temperature on phosphate removal using TPM. C_e: phosphate concentration; E: removal efficiency; (b) effect of dosage on phosphate removal using TPM.

To confirm the feasibility of this removal process, the thermodynamic parameters of phosphate removal onto TPM including free energy (G), enthalpy (H) and entropy (S) were calculated by the equations followed [103]:

$$\Delta G = -RT \ln K_{TPM} \quad (3.9)$$

$$\Delta G = \Delta H - T\Delta S \quad (3.10)$$

where K_{TPM} is the thermodynamic equilibrium constant of the removal process using TPM. It was computed by plotting $ln(q_e/C_e)$ versus q_e and extrapolating q_e to zero. R is the universal gas constant (8.314 J mol^{-1} K^{-1}), T is the temperature (K) of experiment.

The values of ΔH, ΔG and ΔS are summarized in Table 4.4. The negative values of ΔG indicated that the phosphate removal process by TPM adsorption was favorable, spontaneous and endothermic under natural temperature conditions [99]. The values of ΔG decreased from -2.08 kJ mol^{-1} to -3.08 kJ mol^{-1} with the temperature increased from 288.15 K to 308.15 K, indicating more efficient adsorption at higher temperature. The positive values of ΔS revealed that the increasing randomness at the adsorbent-aqueous interface during the phosphate removal onto TPM [50]. Furthermore, the positive values of enthalpy (ΔH) strongly proved the endothermic nature of this removal process, which was high enough to ensure strong interaction between adsorbents and adsorbates. The increase of phosphate removal capacity of TPM under higher temperature may be resulted from the activations or enlargement of pore size of TPM surface [99]. This observation is

similar with the reports when using modified bentonites and aleppo pine as adsorbent, respectively [99, 104].

Table 3.4 Thermodynamic parameters for phosphate adsorption on TPM at initial pH 7, initial phosphate concentration 20 mg L^{-1} and dosage of 4 g L^{-1}.

ΔG (kJ mol^{-1})			ΔS (J mol^{-1} K^{-1})	ΔH (kJ mol^{-1})
288.15 K	298.15 K	308.15 K	49.6	12.1
-2.08	-2.89	-3.08		

3.3.6 Effect of dosage

The effect of dosage on phosphate adsorption is illustrated in Figure 3.4b. The results showed that phosphate removal efficiency increased with the increase of TPM dosage, due to that more surface area and adsorption functional sites were available under higher TPM dosage conditions. The phosphate removal efficiency increased to 94.32% at TPM dosage of 50 g L^{-1}. In contrast, the phosphate adsorption capacity (q_e, mg g^{-1}) decreased with the increase of TPM dose, from 2.385 mg g^{-1} at dosage of 5 g L^{-1} to 0.377 mg g^{-1} at dosage of 50 g L^{-1}, respectively.

In addition, different initial concentration of phosphate seemed to affect q_e which increased under higher initial phosphate concentration even under the same dosage of TPM. For example, q_e was 0.495 mg g^{-1} at initial concentration of 10 mg L^{-1} and increased to 0.836 mg g^{-1} at initial concentration of 20 mg L^{-1}, respectively. The result indicated that the phosphate adsorption saturation could not be reached under lower initial phosphate levels due to lower contact opportunity with TPM surface [95]. In addition, the desirable adsorption onto TPM at higher initial phosphate levels may also be resulted from a greater driving force under higher concentration gradient pressure [105].

3.3.7 Phosphate recycling and TPM regeneration

Based on its un-renewable resource attribute, the reclamation of phosphate from P-adsorbed TPM is a good approach for alleviating the phosphorus shortage.

Moreover, the further application of TPM in practice depends not only on TPM adsorption potential but also on its reusability.

Twenty gram of TPM were dosed in 550 mL of phosphate solution (50 mg L^{-1}). The phosphate adsorbed on TPM was calculated as 1.316 mg $gTPM^{-1}$ through Eq. (2.1) when equilibrium was achieved. The recycling quantities can be estimated by Eq. (3.11):

$$\sum_{i=1}^{n} Q_i = \frac{\sum_{i=1}^{n} C_i V_i}{1000} \tag{3.11}$$

where Q_i (g) is the recycled phosphate from TPM, n is the times of soaking treatment, C_i (mg L^{-1}) and V_i (mL) is the concentration and volume of the eluant, respectively. The procedure of phosphate recycling and TPM recovery is exhibited in Figure 3.5.

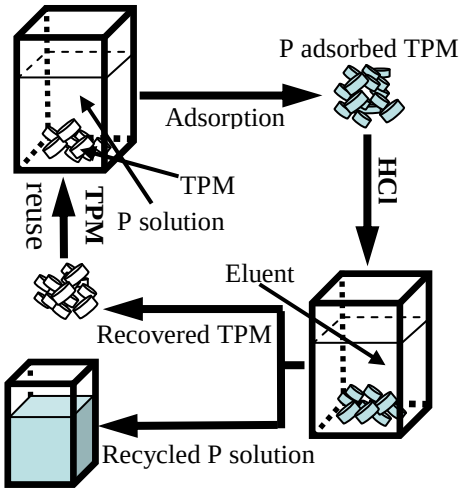

Figure 3.5. The procedure of phosphate recycling and TPM recovery.

The data of phosphate loading on TPM (before and after regeneration) in each cycle are shown in Figure 3.6. The experiment showed that TPM could be recovered under different HCl concentrations and the adsorbed phosphate could be recycled in the recovery process. According to the results, 70.29% of adsorbed phosphate could be totally recycled in 5 cycles when 0.2 mol L^{-1} HCl used as eluant (Figure 3.6a, n = 2, V = 50 mL). The phosphate adsorbed and desorbed was calculated as 4.91 mg and 3.45 mg, respectively. In contrast, 88.85% of phosphate adsorbed could be recycled during 3 cycles when 0.5 mol L^{-1} of HCl were used (Figure 3.6b, n = 1, V = 50mL); but the phosphate adsorbed and desorbed was only 1.88 mg and 1.67 mg, respectively. As the result shown, TPM recovery and phosphate recycling depended on the concentration of H^+ in eluant. H^+ ions might destroy the functional group (-OH) hence the releases of phosphate [57]. In addition, the dissolution of phosphate-metal precipitation might occur under sufficient H^+ ions. The results showed that high HCl concentration had disadvantageous effect on the phosphate removal capacity of TPM. The results also indicated that high concentration of HCl had negative effect on the phosphate removal capacity of TPM. That is an improper concentration of HCl used as eluent would result in a decrease of phosphate removal capacity and recovery cycles. In this study, the removal capacity decreased sharply at 4th cycle and 2nd cycle when 0.2 mol L^{-1} and 0.5 mol L^{-1} HCl used, respectively. This observation implied a higher potential reusability of TPM for phosphate adsorption when 0.2 mol L^{-1} HCl used as eluant. Furthermore, little effect was observed when 0.1 mol L^{-1} NaOH used as eluent, disagreeing with the result of Ramesh et al [106] who used

akaganeite as adsorbent for phosphate removal. This might be attributed to the different compositions between akaganeite and TPM.

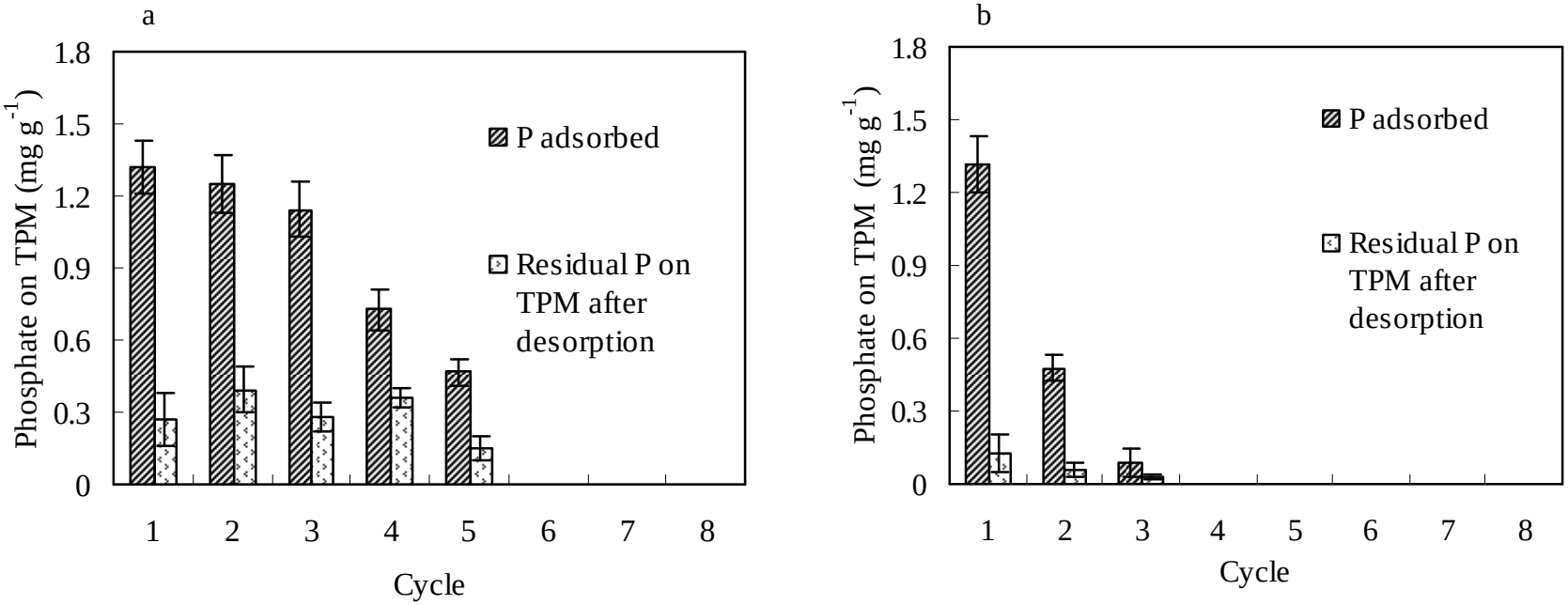

Figure 3.6. TPM recovery and phosphate recycling: (a) Eluant: 0.2 mol L^{-1} HCl; (b) Eluant: 0.5 mol L^{-1} HCl.

3.4 Conclusions

In this study, the TPM developed from Kanuma mud, corn starch and CaO was utilized for phosphate removal. The TPM exhibited excellent phosphate adsorption ability. The Freundlich isotherm model and pseudo-second-order model matched the removal process well. The estimated maximum adsorption capacity was 4.39 mg g^{-1}, better than many other clay mineral adsorbents. The removal process reached its equilibrium in approximately 2 h, and 89.08% of removal process was achieved in the beginning 30 min. Furthermore, phosphate removal efficiency mainly depended on pH and temperature variations. The desirable pH range for phosphate adsorption onto TPM was pH 5.0 - 9.0 and relatively higher temperature could have advantageous effect on the removal efficiency. According to the thermodynamics result, the phosphate removal onto TPM was a spontaneous and endothermic process. In addition, phosphate adsorbed could be recycled using HCl as eluant. The preliminary tests indicated that the recovered TPM could be recycled for 5 times for phosphate removal application under the optimum conditions.

Chapter 4 Electrochemically modified novel tablet porous material developed as adsorbent for phosphate removal from aqueous solution

4.1 Introduction

The wide utilization of P-fertilizers in agriculture and industry enhances the nutrient element load when P residual and waste discharged into water bodies without any treatment. It causes many environmental issues [60, 61], one of the most severe problems is eutrophication in surface water bodies [107]. It causes the deterioration of aquatic ecosystems and the death of aquatic animals [108]. In most cases, phosphorus content is the limiting factor in eutrophication [12]. In a word, the removal of phosphorus has become the focus of investigation by many researchers.

Many techniques have been developed for phosphorus removal such as biological phosphorous removal processes [109], chemical precipitation [63], crystallization [66], electrochemical [110] and membrane bioreactor (MBR) [111]. Among these technologies, Electrochemical (coagulation) method is one worth mentioning because of its high removal efficiency [112], more than 90% of phosphate can be removed under optimum conditions. With regard to electrochemistry, defects are also obvious: such as the difficulty in utilizing it for large amounts of wastewater treatment and the problems of in-situ treatment. The results in chapter 3 showed that effective phosphate removal efficiency could be achieved by adsorption method. In this situation, the combination of electrochemical method and adsorption can be regarded as a good alternative for phosphate removal [113].

Kanuma mud is a kind of geomaterial abundant in Japan. Kanuma mud possesses some functional physical and chemical abilities such as high permeability, water retention property and porosity. In Chapter 3, a tablet porous material (TPM) consisting of Kanuma mud, corn starch, white cement, iron powder and calcium oxide was successfully developed. In this chapter, TPMs were modified by an ESM process and then utilized to remove phosphate. The physical, chemical and surface characteristics, isotherms model, and kinetic model were investigated. In addition, some influencing factors (such as pH, temperature and selectivity) are also discussed.

4.2 Materials and methods

4.2.1 Synthesis of tablet porous material

Kanuma mud was manually smashed and sieved; particle sizes less than 300 μm were selected. Corn starch, white cement, iron powder and CaO (analytical reagent) were supplied by Wako Pure Chemical Industries Ltd, Japan. White cement was supplied by DAISO INDUSTRIES Co., LTD, Japan. The tablet porous material was synthesized using the following steps (the same to Figure. 3.1, Chapter 3): (a) Smashed Kanuma mud, corn starch, iron powder, white cement and CaO were uniformly mixed with a mass ratio of 3: 0.5: 1: 1: 1. (b) Deionized water was then added into the mixture to assist the cohesion process. (c) A granulation procedure was performed on the tablet granules at room temperature. (d) The resulting tablet granules were naturally dried at room temperature for 24 h and then calcined for 1 h in a muffle furnace at 600 ^{o}C.

4.2.2 Preparation and ESM process

A cylindrical electrochemical cell (volume: 500 mL) was designed (Figure 4.1). Two Fe plates were used as the cathode and anode, set at a 10 mm plate distance. The areas of the anode and cathode immersed in the treated solution were both 35 cm^2. A DC potentiostat (Takasago, EX1500H2) with a voltage range of 0 - 240 V and a current range of 0 - 25 A was employed as power supply for ESM process of TPM. A weighed amount (20 g) of TPM was introduced between the two Fe plates, to which was added 0.5 L NaCl solution (electrolyte) with a concentration of 0.25 g L^{-1} at a pH of approximate 6.7. The modification process was performed for 25 - 30 min (current: 0.25 A) and soaked in the electrolyte for 24 h. Finally, the soaked TPM was calcined again in a muffle furnace at 600 ^oC for 30 min and named as electrochemical-TPM (ECTPM).

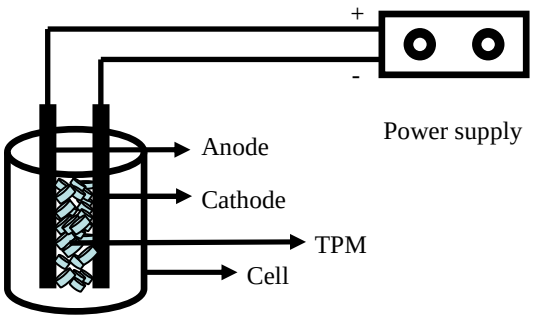

Figure 4.1. Diagram of the electrochemical apparatus.

4.2.3 Phosphate adsorption experiments

A stock solution of 50 mg L^{-1} phosphate was prepared by dissolving KH_2PO_4 (anhydrous, analytical grade) in deionized water. All the adsorption experiments were conducted in triplicate in 50 mL test tubes in a thermostat (298.15K, 303.15K and 308.15K were selected in thermodynamics experiments); all experiments were performed without shaking to simulate practical conditions.

4.2.3.1 Isotherms experiment

A number of 0.2 g ECTPMs were added into test tubes under initial phosphate concentrations range from 5 to 50 mg L^{-1} (50 mL) and initial pH 7.0 respectively. Then the test tubes were set in the thermostat (25 ± 1 ^{o}C).

4.2.3.2 Kinetic experiment

One gram ECTPM was individually dosed into test tubes containing 50 mL of 10 mg L^{-1} phosphate solution. The sampling time intervals were 5, 10, 20, 30, 90, 120 and 180 min, respectively (initial pH 7.0, 25 ± 1 ^{o}C).

4.2.3.3 Effect of pH

50 mL phosphate solutions (10 mg L^{-1}) were added respectively to 11 test tubes with 1 g ECTPM doses. Different volume of 0.1 M HCl and NaOH were dosed to adjust the initial solution pH ranging from 2.0 to 12.0 under stirring by a magnetic stirrer. All the test tubes were capped to avoid evaporation and the pH values were determined after 2 h (25 ± 1 ^{o}C).

4.2.3.4 Thermodynamics and effect of temperature

A series of 5, 10, 15 and 20 mg L^{-1} of phosphate solution were used in this test to evaluate the effect of temperature under conditions of an initial pH of 7.0 and dosage of 4 g ECTPM L^{-1}, and 298.15, 303.15 and 308.15 K were selected for practical purposes.

4.2.3.5 Effect of selectivity.

A series of 5, 10, 15 and 20 mg L^{-1} of phosphate solution were used for adsorption in the presence of different concentration of nitrate (A series of 10, 20, 30, 40 and 50 mg L^{-1}, initial pH 7.0, 25 ± 1 ^{o}C). The selectivity of phosphate adsorption onto ECTPM and TPM was tested.

4.2.4 Analytical methods

ECTPM was characterized by Energy Dispersive X-Ray Spectroscopy (JED-2200, JEOL Ltd, Japan) and scanning electron microscope (Field Emission Scanning Electron Microscope, JSM-6330F, JEOL Ltd, Japan) to obtain its physical, chemical and surface characteristics; Brunauer-Emmett-Teller (BET) specific surface area and BJH pore distribution were obtained by an analysis device (Coulter SA3100, US) using the He-N_2 method. All the equilibrium phosphate concentration was analyzed with the ascorbic acid method (4500-P E) [71].

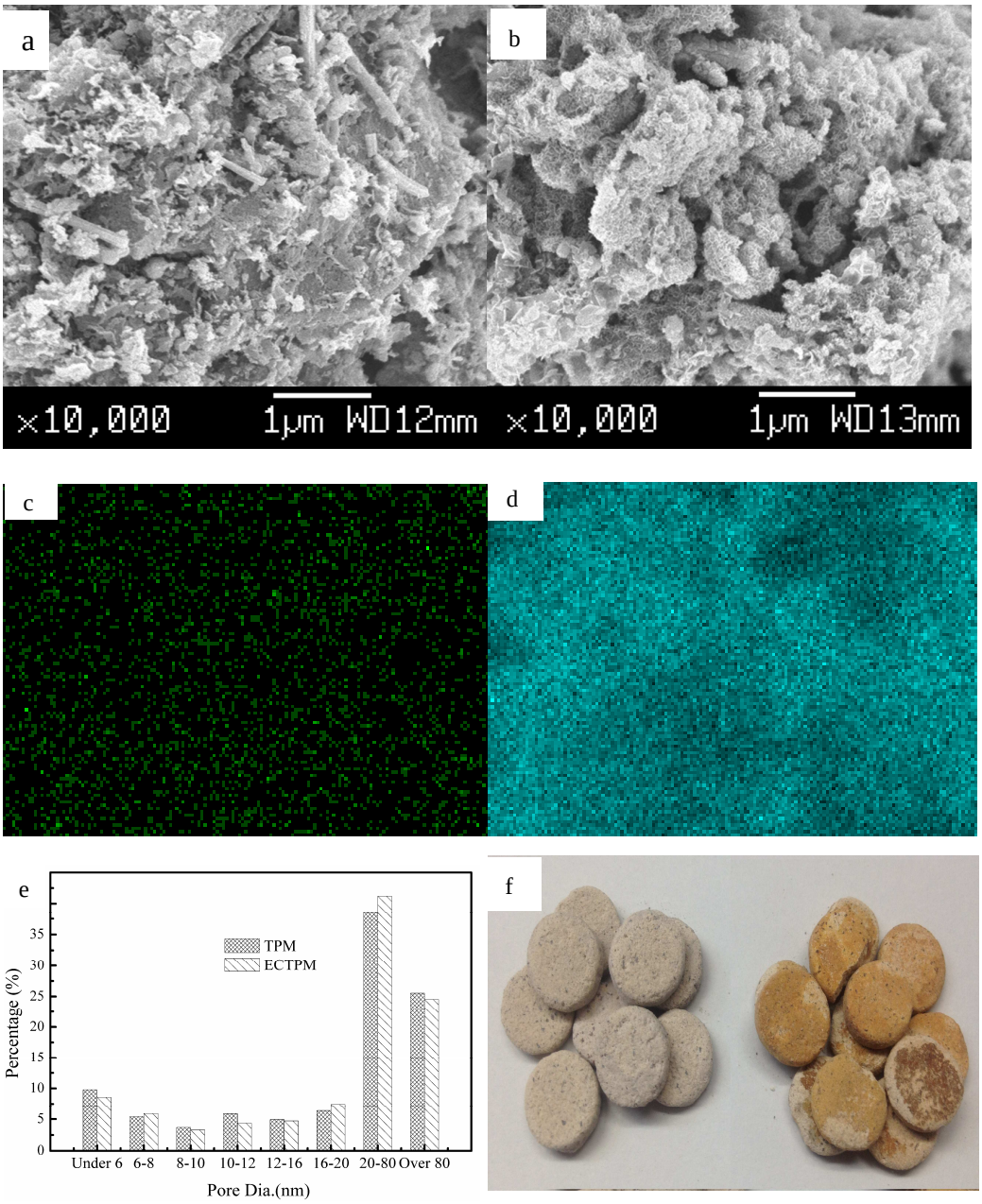

Figure 4.2. Characterization: (a) SEM image of TPM, 10000x; (b) SEM image of electrochemical surface modified TPM (ECTPM), 10000x; (c) Fe mapping of TPM surface, 10000x; (d) Fe mapping of ECTPM surface, 10000x; (e) pore diameter distribution of TPM and ECTPM; (f) photo of pristine TPM (left) and ECTPM (right).

4.3 Results and discussion

4.3.1 Characterization

Figure 4.2a is SEM image of TPM, 10000x; and Figure 4.2b is SEM image of surface modified TPM (ECTPM), 10000x. The images obviously show that micro floc were present widely after surface modification through the ESM process. The reactions could be expressed as [114]:

Reactions at the cathode:

$$3H_2O + 3e^- \rightarrow \frac{3}{2}H_2(gas) + 3OH^- \quad (4.1)$$

Reactions at the anode and surface of TPM:

$$4Fe(solid) \rightarrow 4Fe^{2+}(aqueous) + 8e^- \quad (4.2)$$

At the presence of dissolved oxygen in solution:

$$4Fe^{2+}(aqueous) + 10H_2O(liquid) + O_2(gas) \rightarrow 4Fe(OH)_3 + 8H^+(aqueous) \quad (4.3)$$

Overall reaction in system:

$$4Fe(solid) + 10H_2O(liquid) + O_2(gas) \rightarrow 4Fe(OH)_3(solid) + 4H_2(gas) \quad (4.4)$$

It could be concluded that the Fe-hydroxyl component might bring about these morphological changes to TPM surface during the ESM process. It was proved through Fe mapping. Figure 4.2c shows the Fe mapping of pristine TPM surface, and Figure 4.2d shows the Fe mapping of ECTPM surface, it is obvious that ESM could largely enhance the Fe distribution on the surface of adsorbent. This observation also indicates ECTPM would develop a more positive effect on adsorption sites than that of TPM in phosphate adsorption [55]. Furthermore, the porous texture and structure were increasingly developed at the surface of ECTPM than TPM; suggesting it might

be formed during the ESM process where part of the iron powder was oxided into Fe^{3+} resulting in a porous texture.

The EDX result is shown in Table 4.1. It was obvious that TPM was mainly composed of metal oxides such as Fe_2O_3, Al_2O_3, SiO_2 and CaO. Fe_2O_3 [55] and Al_2O_3 [98] are reported as a good adsorbent for phosphate by surface precipitation, and CaO in TPM can be transformed into calcium hydroxides enhancing the inner-sphere ligand exchange process. Meanwhile, the surface component of ECTPM is much different from TPM, where the mass of Fe obviously increased. This observation is in agreement with the Fe mapping of the adsorbent surface (Figure 4.2c, Figure 4.2d).

The results of specific surface area of TPM and ECTPM (Table 4.1) show that BET surface area is 15.59 $m^2 g^{-1}$ for TPM and increased to 16.12 $m^2 g^{-1}$ for ECTPM, indicating that ESM could slightly enhance the specific surface area of TPM. The specific surface area of ECTPM and TPM was similar with the use of red mud, 14.09 $m^2 g^{-1}$ [94] but lower than hydrotalcite, 44 $m^2 g^{-1}$ [60]. In addition, the BJH pore size distribution (Figure 4.2e) indicates that ECTPM and TPM is still a typical mesoporous material according to IUPAC classification [73], and ESM could slightly enhance the pore volume. Furthermore, the higher mass ratio of corn starch used as a pore-enhancer was major means to increase the pore volume of TPM, but the structure stability of TPM would decrease with the increase in mass ratio of corn starch. In this study, the 0.5/6.5 mass ratio of pore-enhancer was desirable in the TPM synthesis process.

Table 4.1 The results of BET and EDX analysis for ECTPM and TPM

Sample	BET surface area		Total pore Volume
	Values (m^2 g^{-1})	Monolayer volume (mL g^{-1})	Values (mL g^{-1})
TPM	15.59	4.13	0.0974
ECTPM	16.12	4.25	0.1057

Results of EDX analyasis

Content (%)	Fe_2O_3	MgO	Al_2O_3	SiO_2	CaO
TPM	25.1	8.0	21.5	26.2	19.2
ECTPM	31.7	6.8	19.7	23.8	18.0

4.3.2 Adsorption isotherms

The equilibrium uptake capacity of phosphate, q_e (mg g^{-1}), was calculated by the Eq. (2.1). In order to examine the maximum phosphate adsorption capacity of ECTPM and TPM, Langmuir and Freundlich isotherm models were applied to fit the experimental data, which can be described as Eq. (2.2) and Eq. (2.3), respectively [115].

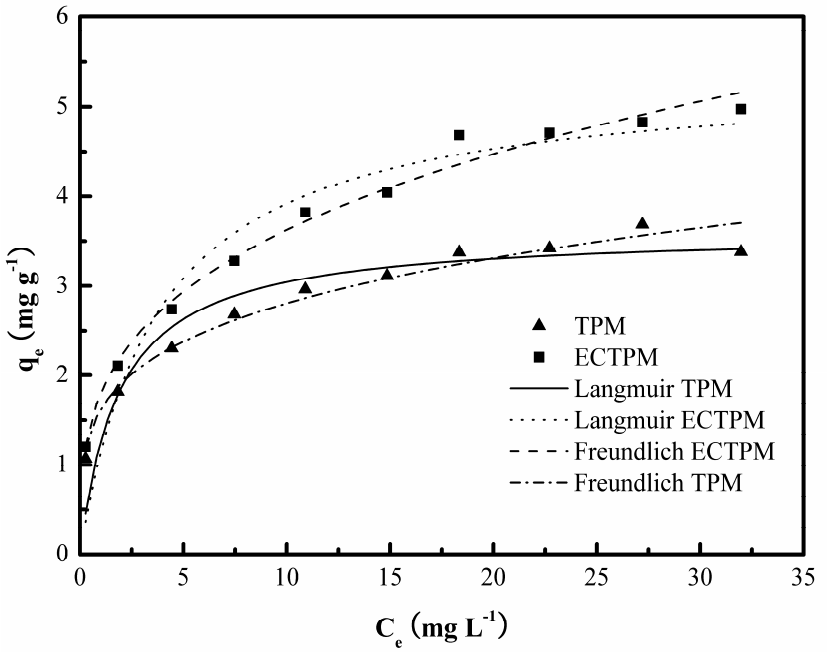

Figure 4.3. The curve of the Langmuir and Freudlich models for phosphate adsorption on TPM and ECTPM. Initial P concentration: 5 to 50 mg L^{-1}. Temperature: 25 ± 1 ^{o}C. Dosage: 4 g L^{-1}.

Table 4.2 The parameters and constants of Langmuir and Freundlich models for phosphate adsorption on TPM and ECTPM.

	Langmuir model			Freundlich model		
	q_{max} (mg g^{-1})	b (L mg^{-1})	R^2	K_f (mg g^{-1})	n	R^2
TPM	3.61	0.535	0.901	1.62	4.187	0.973
ECTPM	5.36	0.271	0.924	1.77	3.231	0.988

The Langmuir model is often used to exhibit a monolayer distribution of solute within the adsorbent and the Freundlich isotherm model usually tends to describe a complex heterogeneous adsorption process assuming that different functional sites with several adsorption energies were heterogeneous [75].

The parameters and constants of Langmuir and Freundlich models for phosphate adsorption on TPM and ECTPM are summarized in Table 4.2. Figure 4.3 is the curve of Langmuir and Freundlich model for phosphate adsorption on TPM and ECTPM. Both of R^2 obtained from the Langmuir and Freundlich models were over 0.90; indicating a good mathematical match by both models. The correlation coefficient of the Freundlich model (0.973 of TPM and 0.988 of ECTPM, respectively) were higher than those of the Langmuir model, indicating that the phosphate adsorption through TPM or ECTPM seems to a multilayer adsorption process with several adsorption energetic distributions of functional sites and with interaction between adsorbed solute.

The estimated maximum adsorption capacity of TPM and ECTPM were 3.61 and 5.36 mg g^{-1}, respectively. It is obvious that ESM process used as a modification method could enhance adsorption abilities of TPM on phosphate removal. In addition, K_f is an indicator of adsorption capacity and n indicates the effect of concentration on the adsorption capacity and represents the adsorption intensity (dimensionless). A higher value of n ($n > 1$) indicates favorable adsorption. It was also found that the TPM and ECTPM are superior to other natural clay mineral (mud) adsorbents based

on their maximum phosphate adsorption capacities (Figure 4.4a), implying that TPM or ECTPM has the potential for phosphate removal from wastewater in practice.

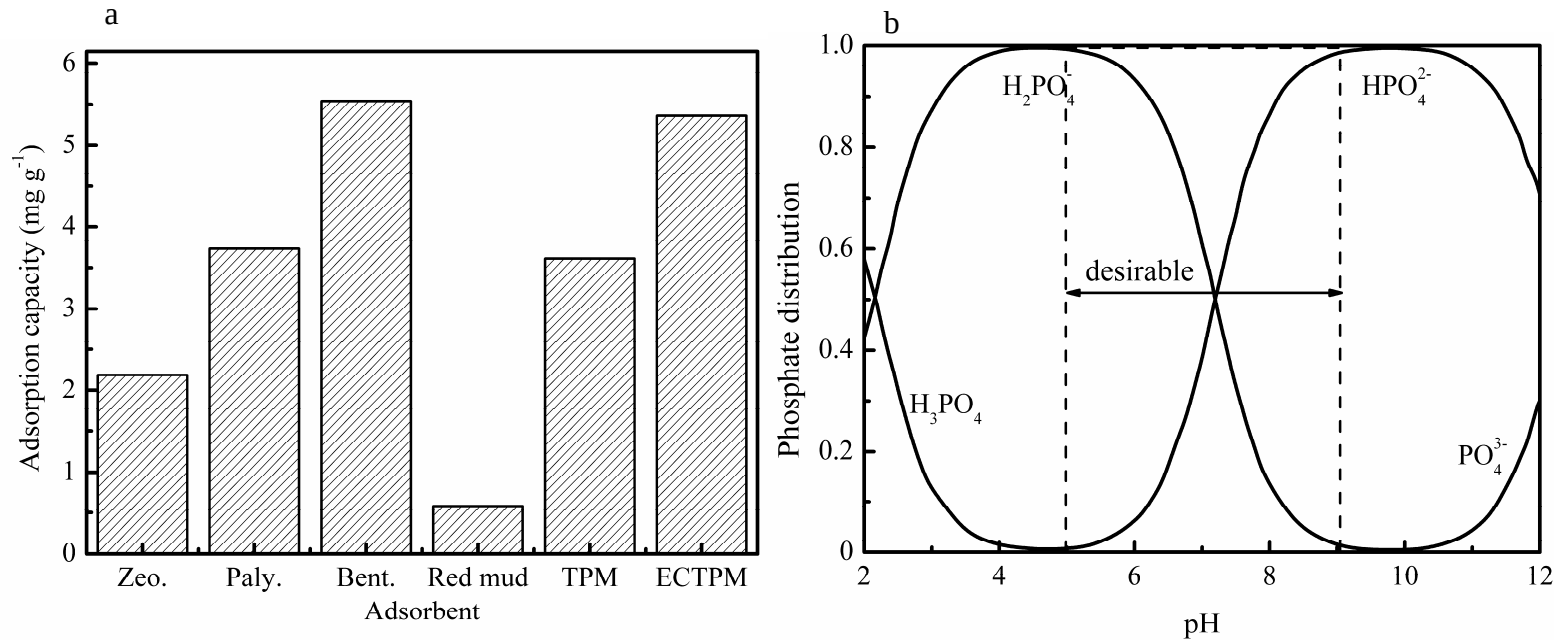

Figure 4.4. (a) Comparison of maximum phosphate adsorption capability between ECTPM (TPM) and other mineral adsorbents. Zeo.: Na-natural zeolite [72]; Paly.: Natural palygorskite [53]; Bent.: Bentonite [99]; Red mud [76]. (b) Distribution diagram for phosphate present as different protonated species as a function of pH [80].

4.3.3 Effect of contact time and kinetics

A kinetics study is important to evaluate the adsorption process and it can provide further information on the process mechanisms. In this study, a pseudo first-order model and pseudo second-order model were applied to examine the kinetics of phosphate adsorption onto TPM and ECTPM.

The pseudo first-order model is expressed as Eq. (2.4) [77] and can be simplified as Eq.(2.5) after integration with the boundary conditions being set ($q_t = 0$ and q_t when $t = 0$ and t, respectively). The pseudo second-order model is expressed as Eq. (2.6), which can be simplified as Eq. (2.7).

The effect of contact time on phosphate adsorption is shown in Figure 4.5. It is obvious that the phosphate removal process onto TPM and ECTPM reflect a three-step natural process: a fast reaction step at 0 - 45 min; a low reaction step at 45 - 120 min and an equilibrium step after 120 min. The fast step is similar to the report by Fox et al [100] who undertook experiments using river sediment, but much faster than other materials like modified bentonites [99]. 96.37 % of the removal process was finished in the first step (during the first 45 min). In this step, phosphate seemed to be removed through surface adsorption [67], and more available vacant adsorption sites supplied advantageous effects on this removal process [60]. The slow step occurred from the 45 min to 120 min. Only a small amount of phosphate was removed in this step mainly due to the decrease of vacant adsorption sites on the surface of TPM. The equilibrium was achieved at the 120 min, no further removal efficiency reflected in the equilibrium step (Step 3).

The constants of the pseudo first-order model and pseudo second-order model are given in Table 4.3, and the pseudo second-order model plots of phosphate adsorption are shown in Figure 4.5. Based on the correlation coefficients obtained, it is clear that the phosphate adsorption process onto TPM and ECTPM could be well described by pseudo second-order model under the experimental conditions.

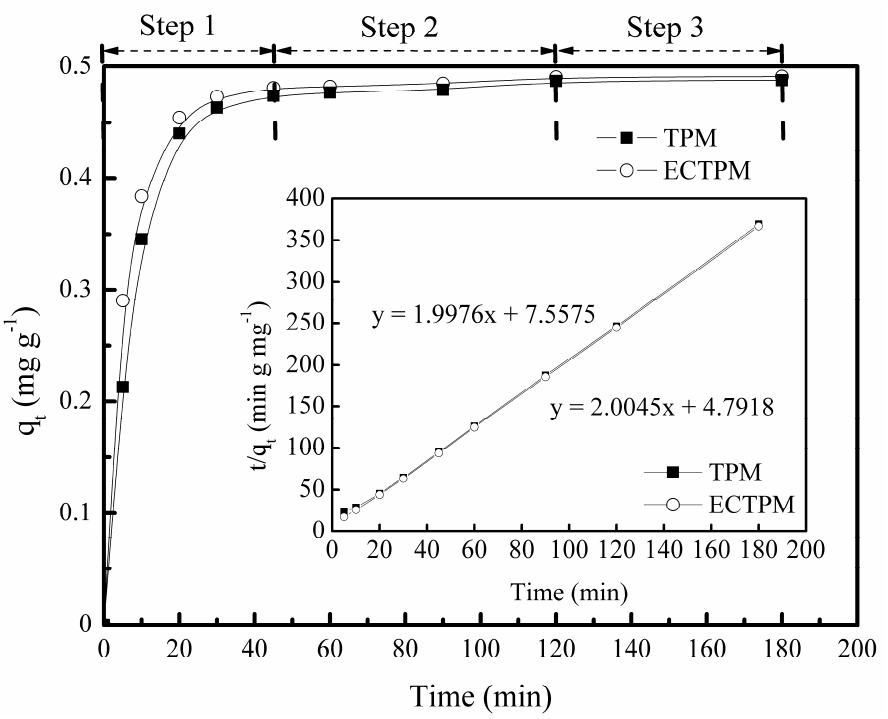

Figure 4.5. The effect of contact time on phosphate adsorption by TPM and ECTPM (lower inset shows pseudo second-order model plot of phosphate adsorption).

Initial P concentration: 10 mg L^{-1}. Temperature: 25 ± 1 ^{o}C. Dosage: 20 g L^{-1}.

Table 4.3 The constants of kinetic models for phosphate adsorption on TPM and ECTPM.

	Pseudo first-order model			Pseudo second-order model		
	q_e (mg g^{-1})	k_1 (min^{-1})	R^2	q_e(mg g^{-1})	k_2 (g (mg min) $^{-1}$)	R^2
TPM	0.776	0.0123	0.865	0.499	0.538	0.999
ECTPM	0.125	0.0162	0.933	0.501	0.838	0.999

4.3.4 Removal mechanism and the effect of pH

Phosphate dissociation equilibrium in aqueous solution are pH-dependent, which can be presented as [97]:

$$H_2PO_4^- + H_2O = H_3PO_4 + OH^- \quad (4.5)$$

$$HPO_4^{2-} + H_2O \leftrightarrow H_2PO_4^- + OH^- \quad (4.6)$$

$$PO_4^{3-} + H_2O \leftrightarrow HPO_4^{2-} + OH^- \quad (4.7)$$

$$H_2O = H^+ + OH^- \quad (4.8)$$

These protonation reactions are summarized in Figure 4.4b. Clearly, with pHs ranging from 5 to 10, the majority species are $H_2PO_4^-$ and HPO_4^{2-}. For a detailed description, the $H_2PO_4^-$ prevailed when pH ranged from 5 to 7 and the concentration of HPO_4^{2-} is higher when pH ranged from 7 to 10; For pH ranging from 10 to 12, HPO_4^{2-} dominated than PO_4^{3-} and PO_4^{3-} becomes significant when pH is higher than 12. Metals mainly exist as oxides and hydroxides in TPM, which could provide adsorption sites for phosphate. It is well known that phosphate is usually considered to be removed through an inner-sphere ligand exchange mechanism [81].

Considering that different phosphate species dominate in different pH solutions, the following reactions may be included in phosphate removal through TPM adsorption [55]:

$$\equiv MOH + PO_4^{3-} + H^+ \Leftrightarrow \equiv MPO_4^{2-} + H_2O \quad (4.9)$$

$$\equiv MOH + PO_4^{3-} + 2H^+ \Leftrightarrow \equiv MPO_4H^- + H_2O \quad (4.10)$$

$$\equiv MOH + PO_4^{3-} + 3H^+ \Leftrightarrow \equiv MPO_4H_2 + H_2O \quad (4.11)$$

In addition, phosphate-metal precipitation reaction seems to be an alternative explanation. It can be presented as:

$$3M^{x+} + xPO_4^{3-} = M_3(PO_4)_x \quad (4.12)$$

where M is metal component, such as Al, Fe, Ca, Si, etc.

Eq. (4.1) to Eq. (4.4) clearly shows that ESM could enhance the quantities of functional groups (-OH and Fe^{3+}), thus a higher phosphate adsorption capacity onto ECTPM could occur than for TPM.

Figure 4.6 shows the results of phosphate removal by TPM and ECTPM adsorption under different initial solution pH. It is obvious that the phosphate adsorption capacity of ECTPM was higher than that of TPM, indicating that more -OH and Fe^{3+} due to the ESM process could enhance the adsorption capacity. In addition, Figure 4.6 also shows that pH change plays a significant effect on phosphate removal through TPM and ECTPM adsorption. The equilibrium phosphate removal efficiency remained almost unchanged (slightly varied within 90.35 - 93.04% onto ECTPM and 87.95 - 90.49% onto TPM, respectively.) within solution pH range from 5.0 to 9.0. Figure. 4.6 and Eq. (4.6) shows that the dominant phosphate species should be $H_2PO_4^-$ (monovalent dihydrogen phosphate) and HPO_4^{2-} (divalent hydrogen phosphate) when pH varied within 5.0 to 9.0, indicating that $H_2PO_4^-$ and HPO_4^{2-} could be well adsorbed by TPM and ECTPM (Eq. (4.10) and (4.11)). The optimum pH value for phosphate removal was around pH 6.0. This result agrees with those of M. Özacar [83] and Yan et al [99] who used alunite and Fe-Al modified bentonite as phosphate absorbent, respectively. It is known that extreme pH conditions are scarcely

encountered in natural surface water bodies or wastewater treatment plants, thus ECTPM and TPM could be used in practice without pH adjustment and the ESM process was also proved to be a novel feasible surface modification process.

The phosphate removal efficiency decreased with further increase in solution pH and sharply decreased when pH higher than 10.0. At pH 12.0, the P removal efficiency reduced to 71.10% and 66.28% onto ECTPM and TPM, respectively, possibly caused by the deprotonation of oxide/hydroxides under higher pH conditions which could be expressed by following equation:

$$\equiv M - OH \rightarrow \equiv M - O^{-} + H^{+} \quad (4.13)$$

This process may result in a negative change of surface charge of ECTPM and TPM hence the decrease of phosphate removal efficiency. In addition, the functional group (-OH) may be destroyed in the deprotonation process, leading to phosphate release and decrease in phosphate adsorption because of electrostatic repulsion. Furthermore, the competitive adsorption of OH^{-} ions probably plays an important role under high pH conditions.

On the other hand, phosphate removal efficiency exhibited a decreasing trend with the decrease in solution pH when the pH was lower than 3.0 (Figure 4.6), which reduced to 51.33 % onto ECTPM and 47.89% onto TPM at pH 2.0, respectively. Eq. (4.12) showed that the dominant phosphate species in the solution were $H_2PO_4^-$ and H_3PO_4 when pH was lower than 3.5 (Figure 4.6). As mentioned above, $H_2PO_4^-$ could be removed effectively by ECTPM and TPM; it is assumed that H_3PO_4 seems unable to be adsorbed onto ECTPM and TPM surfaces considering the decrease in removal

efficiency. Further, under extremely low pH conditions, metal oxides/hydroxides might become unstable and start to dissolve because of large amount of H^+ coexisted in the solution, resulting in the decrease of adsorption sites for phosphate adsorption.

Figure 4.6 also shows the comparison of pH change between initial pH and equilibrium pH. It is well known that the process of ligand exchange could enhance the pH value of the adsorbate-liquid system which is caused by the release of OH^- and the consumption of H^+ [81]. Further, the release of OH^- may also be attributed to a metal oxidation hydrolyze, which can be described by following equation [82]:

$$M_xO_y + yH_2O \rightarrow xM^{(2y/x)+} + 2yOH^- \quad (4.14)$$

In this study, it could be easily observed that equilibrium pH was much higher than initial pH after the phosphate adsorption process onto ECTPM and TPM, strongly proving that a ligand ion exchange process and metal oxidations hydrolyze might occur during the adsorption process. The results also shows that more OH^- (higher pH) exist in solution when ECTPM are used as adsorbent than that of TPM, implying the ESM process is an effective method on adsorbent surface modification.

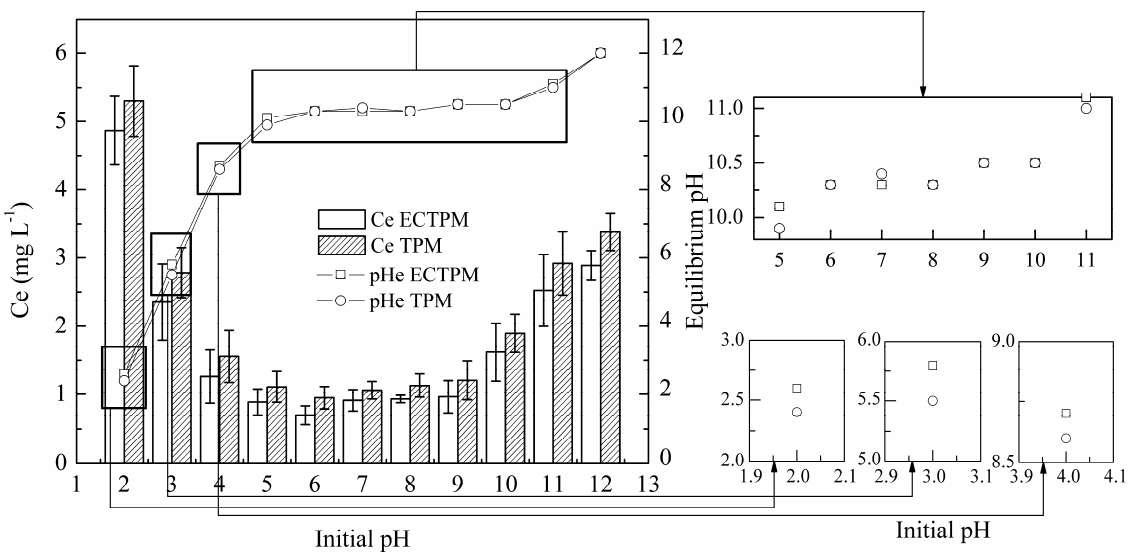

Figure 4.6. The effect of pH change on phosphate adsorption. pH_e: equilibrium pH. Dosage: 20 g L^{-1}. Temperature: 25 ± 1 ^{o}C.

4.3.5 Thermodynamics and effect of temperature

To confirm the feasibility of this removal process, the thermodynamic parameters of phosphate removal onto ECTPM and TPM should be considered. K_T is the thermodynamic equilibrium constant of the removal process using ECTPM and TPM, it was computed using the method of Lyubchik et al [116] by plotting $ln(q_e/C_e)$ versus q_e and extrapolating q_e to zero. The change in Gibbs free energies (ΔG) was then calculated with Eq. (15). Enthalpy (ΔH) and entropy (ΔS) were calculated from the slope and intercept of the plot of lnK_T versus $1/T$ using Eq. (16). R is the universal gas constant (8.314 J mol^{-1} K^{-1}), T is the temperature (K) of experiment [103].

$$\Delta G = -RT \ln K_T \tag{4.15}$$

$$\ln K_T = \frac{\Delta S}{R} - \frac{\Delta H}{RT} \tag{4.16}$$

The values of ΔH, ΔG and ΔS are summarized in Table 4. The negative values of ΔG indicated that the phosphate removal process by TPM adsorption was favorable and spontaneous under natural temperature conditions [99]. The values of ΔG decreased from -2.81 kJ mol^{-1} to -3.08 kJ mol^{-1} onto TPM and from -3.21 to -3.72 kJ mol^{-1} onto ECTPM with the temperature increased from 298.15 K to 308.15 K, respectively, indicating more efficient adsorption at higher temperature. The ΔG values of ECTPM are more negative than that of TPM implying that the reaction occurs easier onto ECTPM than TPM. The positive values of ΔS revealed that the increasing randomness at the adsorbent-aqueous interface during the phosphate removal onto TPM [50]. Furthermore, the positive values of enthalpy (ΔH) strongly prove the endothermic nature of this removal process, which was high enough to

ensure strong interaction between adsorbents and adsorbates. The reaction enthalpy onto ECTPM is much higher than that of TPM, indicating that ECTPM have more chance to interact with adsorbates than TPM. The increase of phosphate removal capacity of ECTPM and TPM under higher temperature may be resulted from the activation or enlargement of pore size of TPM surface [99]. This observation is similar with the reports when using modified bentonites and aleppo pine as adsorbent, respectively [99, 104]. Further, the results of thermodynamics also indicate that ESM process is a feasible technique for adsorbent surface modification.

Table 4.4 The parameters of thermodynamic for phosphate adsorption on TPM and ECTPM.

	ΔG (kJ mol^{-1})			ΔS (J mol^{-1} K^{-1})	ΔH (kJ mol^{-1})
Temp.(K)	298.15	303.15	308.15		
TPM	-2.81	-2.89	-3.08	26.41	5.08
ECTPM	-3.21	-3.46	-3.72	51.64	12.19

4.3.6 Selectivity

In natural surface water, the anion component is always complicated. Nitrate (NO_3^-) widely exists in surface water. The adsorption affinity of phosphate and NO_3^- has been investigated using simulated wastewater. Further the effect of ionic strength should be considered. The adsorption affinity is often represented in term of the distribution coefficient, K_d (mL g^{-1}), which can be calculated as [117]:

$$K_d = \frac{(C_0 - C_e)}{C_e} \times \frac{V}{M} \tag{4.17}$$

where C_0 and C_e are the initial and equilibrium concentration of phosphate in the solution. V is the volume of solution (mL), and M is the mass of adsorbent in grams. The distribution coefficient expresses the chemical binding affinity of phosphate ion to the adsorbent. A higher K_d value indicates a stronger binding affinity. The K_d values of phosphate in the presence of NO_3^- are shown in Figure 4.7.

Figure 4.7 shows that K_d values slightly decreased in the presence of NO_3^- than in its absence in solution, and K_d was further decreased with the increase of NO_3^- concentration. This observation indicates that phosphate adsorption onto ECTPM and TPM would be affected in the present of NO_3^- especially in a low initial phosphate concentrations. Generally speaking, more than one order of magnitude change of K_d values imply a strong affect due to the presence of competing ions, the K_d changing in the same order of magnitude always indicates a slight or no affect when competition ions exist. In this study, K_d changed within one order of magnitude indicating phosphate adsorption onto ECTPM and TPM would not be affected when large amounts of NO_3^- coexist in solution, it was further approved that equilibrium

concentration of NO_3^- was almost same with that of initial (data not shown), and implies that ECTPM (TPM) have good adsorption selectivity on phosphate. Similar observation was obtained with the reports when using goethite [106] and modified palygorskite [53] as adsorbent, respectively.

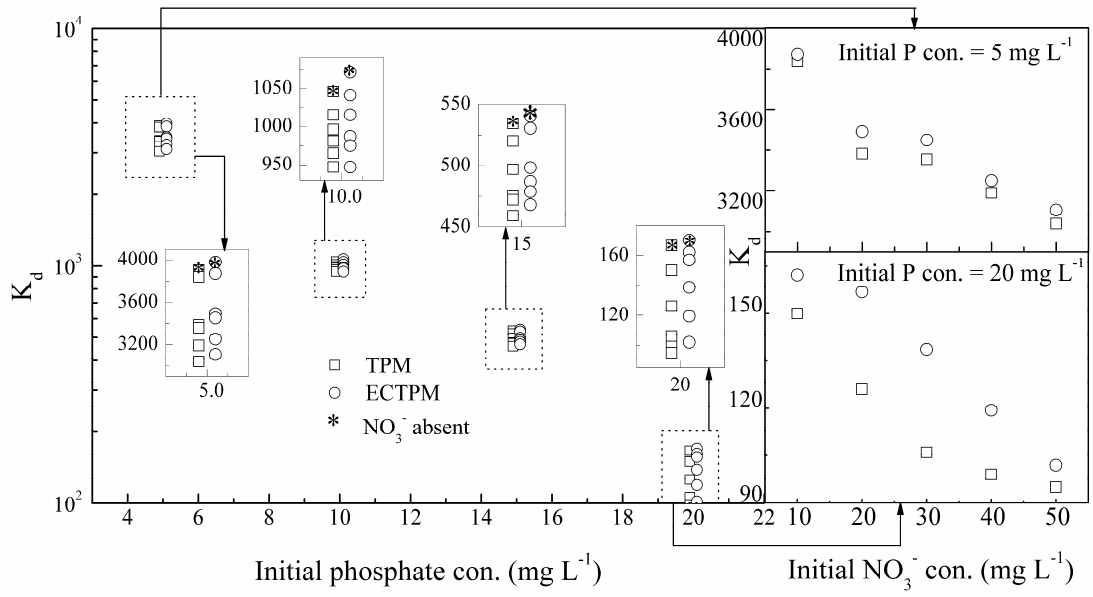

Figure 4.7. Variation in the distribution of coefficients of phosphate in the presence of NO_3^-. Initial P concentration: 5, 10, 15 and 20 mg L^{-1}. Initial NO_3^--N concentration: 10, 20, 30, 40 and 50 mg L^{-1}.

(The variation range of K_d implies the selectivity of adsorbate (P) when competition ions (NO_3^--N) coexisted in liquid phase (lower variation of K_d implies a better selectivity). In this study, the varitation range of K_d is limited within one order of magnitude indicates a excellent P selectivity through TPM and ECTPM.)

4.4 Conclusions

In this study, the TPM developed from Kanuma mud, corn starch, iron powder, white cement and CaO was modified through an ESM process (ECTPM), and then utilized for phosphate removal. The TPM and ECTPM exhibited excellent phosphate adsorption ability. The Freundlich isotherm model and pseudo-second-order model matched the removal process well. The estimated maximum adsorption capacity was 3.61 mg g^{-1} onto TPM and 5.36 mg g^{-1} onto ECTPM, respectively, better than many other clay mineral adsorbents. The removal process reached its equilibrium in approximately 2 h, and 96.38 % of the removal process was achieved in the first 30 min. Furthermore, phosphate removal efficiency depended mainly on pH and temperature variations. The desirable pH range for phosphate adsorption onto TPM was 5.0 - 9.0 and a relatively higher temperature could have advantageous effect on removal efficiency. According to the thermodynamic results, the phosphate removal onto TPM was a spontaneous and endothermic process. In addition, ECTPM and TPM have good adsorption selectivity on phosphate. ECTPM and TPM could be utilized for phosphate removal from aqueous solution and the ESM process could also be applied for adsorbent surface modification.

Chapter 5 Conclusions and suggestions

In the present study, a novel tablet porous material (TPM) was developed from Kanuma mud (K- mud), corn starch, iron powder, white cement and calcium oxide. Followed, an electrochemical surface modification (ESM) method was developed for surface modification on TPM. According to this research, the following conclusions can be obtained:

5.1 Phosphate removal using Kanuma mud

(1) Kanuma mud exhibited certain phosphate adsorption ability;

(2) The adsorption process consisted of a fast and a slow process, the former finished in 110 min;

(3) The Freundlich isotherm model and pseudo-second-order model can well describe the sorption process. The adsorption amount was the best at pH of 6 and comparatively low temperature can enhance the adsorption efficiency;

(4) Phosphate on the absorbent could be hardly desorbed;

(5) The absorbed absorbent can be used as soils fertilization.

5.2 Phosphate removal using developed TPM

(1) The TPM exhibited excellent phosphate adsorption ability; the estimated maximum adsorption capacity was 4.39 mg g^{-1};

(2) The Freundlich isotherm model and pseudo-second-order model matched the removal process well;

(3) The removal process reached its equilibrium in approximately 2 h, and 89.08% of removal process was achieved in the beginning 30 min;

(4) The desirable pH range for phosphate adsorption onto TPM was pH 5.0 - 9.0;

(5) Relatively higher temperature could have advantageous effect on the removal efficiency;

(6) Phosphate removal onto TPM was a spontaneous and endothermic process;

(7) Phosphate adsorbed could be recycled using HCl as eluant.

5.3 Phosphate removal using ESM modified TPM

(1) The ECTPM exhibited excellent phosphate adsorption ability; the estimated maximum adsorption capacity was 5.36 mg g^{-1} onto ECTPM higher than that of TPM;

(2) The Freundlich isotherm model and pseudo-second-order model matched the removal process well;

(3) The removal process reached its equilibrium in approximately 2 h;

(4) The desirable pH range for phosphate adsorption onto TPM was 5.0 - 9.0;

(5) Relatively higher temperature could have advantageous effect on removal efficiency. Phosphate removal onto TPM was a spontaneous and endothermic process;

(6) The ESM process could also be applied for adsorbent surface modification.

5.4 Future research suggestion

In this research, the following study should focus on:

(1) Novel modification method development;

(2) Content adjusting and optimum for TPM production;

(3) Method evaluation for P-recycling (crystallization)；

(4) Development of crystallization seeds for P-recycling；

(5) TPM application in surface water bodies and performance evaluation.

References

[1] World Water Commission, A Water Secure World: Vision for Water, Life and the Environment, World Water Council, Marseille, 2000, 11-19.

[2] J.B. Zedler, S. Kercher, Wetland resources: Status, trends, ecosystem services, and restorability, Annual Review of Environment and Resources, 30 (2005), 39-74.

[3] V.B. Smith, C.H. David, M.B. Cardenas, Z.L. Yang, Climate, river network, and vegetation cover relationships across a climate gradient and their potential for predicting effects of decadal-scale climate change, Journal of Hydrology, 488 (2013) 101-109.

[4] M. Schaefer, Water technologies and the environment: Ramping up by scaling down, Technology in Society, 30 (2008) 415-422.

[5] World Bank, World Development Report 1992: Environment and Development, World Bank, New York, 1992, 100-103.

[6] Water Infrastructure Network, Clean & Safe Water for the 21st Century, A Renewed National Commitment to Water and Wastewater Infrastructure, Water Infrastructure Network, 2000, 1-3.

[7] M.Tiemann, C.Copeland, Water Infrastructure Needs and Investment: Review and Analysis of Key Issues, Congressional Research Service, 2010, 9-11.

[8] L. Smedema, S. Abdel-Dayem, W. Ochs, Drainage and Agricultural Development, Irrigation and Drainage Systems, 14 (2000) 223-235.

[9] R. Hirji, R. Davis, Water Resources and Environmental Technical Note E.1: Irrigation and Drainage Development, The World Bank Washington, D.C., 2003, 9.

[10] A. Avni, M.A. Blázquez, Can plant biotechnology help in solving our food and energy shortage in the future?, Current Opinion in Biotechnology, 22 (2011) 220-223.

[11] O. Hisao, The life element: about phosphorus resources, Journal of Bioscience and Bioengineering, 90 (2012) 464-492.

[12] F.J. Fernández, J. Villasenor, L. Rodríguez, Effect of the internal recycles on the phosphorus removal efficiency of a WWTP, Industrial & Engineering Chemistry Research, 46 (2007) 7300-7307.

[13] G.K. Morse, S.W. Brett, J.A. Guy, J.N. Lester, Review: Phosphorus removal and recovery technologies, Science of The Total Environment, 212 (1998) 69-81.

[14] Y. Liu, H. Shi, W. Li, Y. Hou, M. He, Inhibition of chemical dose in biological phosphorus and nitrogen removal in simultaneous chemical precipitation for phosphorus removal, Bioresource Technology, 102 (2011) 4008-4012.

[15] T. Clark, T. Stephenson, P.A. Pearce, Phosphorus removal by chemical precipitation in a biological aerated filter, Water Research, 31 (1997) 2557-2563.

[16] M. Gómez, L. Dvořák, I. Růžičková, J. Wanner, M. Holba, E. Sykorová, Influence of phosphorus precipitation on permeability and soluble microbial product concentration in a membrane bioreactor, Bioresource Technology, 129 (2013) 164-169.

[17] Y. Comeau, K.J. Hall, R.E.W. Hancock, W.K. Oldham, Biochemical model for enhanced biological phosphorus removal, Water Research, 20 (1986) 1511-1521.

[18] H. Temmink, B. Petersen, S. Isaacs, M. Henze, Recovery of biological phosphorus removal after periods of low organic loading, Water Science and Technology, 34 (1996) 1-8.

[19] H. Jang, S.H. Kang, Phosphorus removal using cow bone in hydroxyapatite crystallization, Water Research, 36 (2002) 1324-1330.

[20] Y.H. Song, D. Donnert, U. Berg, P.G. Weidler, R. Nueesch, Seed selections for crystallization of calcium phosphate for phosphorus recovery, Journal of Environmental Sciences, 19 (2007) 591-595.

[21] S. Karaca, A. Gurses, M. Ejder, M. Acikyildiz, Adsorptive removal of phosphate from aqueous solutions using raw and calcinated dolomite, Journal of Hazardous Materials, 128 (2006) 273-279.

[22] A. Genz, A. Kornmüller, M. Jekel, Advanced phosphorus removal from membrane filtrates by adsorption on activated aluminium oxide and granulated ferric hydroxide, Water Research, 38 (2004) 3523-3530.

[23] C.T. Hsieh, I.L. Chen, W.Y. Chen, J.P. Wang, Synthesis of iron phosphate powders by chemical precipitation route for high-power lithium iron phosphate cathodes, Electrochimica Acta, 83 (2012) 202-208.

[24] P.H. Hsu, Precipitation of phosphate from solution using aluminum salt, Water Research, 9 (1975) 1155-1161.

[25] L.G. Greenburg AE, Kauffman WJ, The effect of phosphorus removal on the activated sludge process, Sewage and Industrial Wastes, 27 (1955) 277.

[26] S.J. Levin GV, Metabolic uptake of phosphorus by wastewater organisms, Journal of the Water Pollution Control Federation, 37 (1965) 800-821.

[27] D. Gkisberg, Phosphorus Removal from Wastewater, Chemie Ingenieur Technik, 64 (1992) 585-586.

[28] Y. Jaffer, T.A. Clark, P. Pearce, S.A. Parsons, Potential phosphorus recovery by struvite formation, Water Research, 36 (2002) 1834-1842.

[29] E.H. Kim, D.W. Lee, H.K. Hwang, S. Yim, Recovery of phosphates from wastewater using converter slag: Kinetics analysis of a completely mixed phosphorus crystallization process, Chemosphere, 63 (2006) 192-201.

[30] M.M. Seckler, O.S.L. Bruinsma, G.M. Van Rosmalen, Phosphate removal in a fluidized bed—I. Identification of physical processes, Water Research, 30 (1996) 1585-1588.

[31] D. Donnert, M. Salecker, Elimination of phosphorus from municipal and industrial waste water, Water Science and Technology, 40 (1999) 195-202.

[32] M.M. Seckler, M.L.J. van Leeuwen, O.S.L. Bruinsma, G.M. van Rosmalen, Phosphate removal in a fluidized bed—II. Process optimization, Water Research, 30 (1996) 1589-1596.

[33] S. Yim, E.H. Kim, A Comparative Study of Seed Crystals For The Phosphorus Crystallization Process, Environmental Technology, 25 (2004) 741-750.

[34] J. Zoltek Jr., Phosphorus removal by orthophosphate nucleation, Journal of the Water Pollution Control Federation, 46 (1974) 2498-2520.

[35] Y.S. Al-Degs, M.I. El-Barghouthi, A.H. El-Sheikh, G.M. Walker, Effect of solution pH, ionic strength, and temperature on adsorption behavior of reactive dyes on activated carbon, Dyes and Pigments, 77 (2008) 16-23.

[36] K.G. Babi, K.M. Koumenides, A.D. Nikolaou, C.A. Makri, F.K. Tzoumerkas, T.D. Lekkas, Pilot study of the removal of THMs, HAAs and DOC from drinking water by GAC adsorption, Desalination, 210 (2007) 215-224.

[37] J.J.G.M. van Bokhoven, Refinement of a calorimetric method of measuring heats of adsorption and a comparison with an alternative method, Thermochimica Acta, 86 (1985) 257-271.

[38] Q.S. Liu, T. Zheng, P. Wang, J.P. Jiang, N. Li, Adsorption isotherm, kinetic and mechanism studies of some substituted phenols on activated carbon fibers, Chemical Engineering Journal, 157 (2010) 348-356.

[39] A. Halajnia, S. Oustan, N. Najafi, A.R. Khataee, A. Lakzian, The adsorption characteristics of nitrate on Mg-Fe and Mg-Al layered double hydroxides in a simulated soil solution, Applied Clay Science, 70 (2012) 28-36.

[40] H. Deng, J. Lu, G. Li, G. Zhang, X. Wang, Adsorption of methylene blue on adsorbent materials produced from cotton stalk, Chemical Engineering Journal, 172 (2011) 326-334.

[41] M. Doğan, Y. Özdemir, M. Alkan, Adsorption kinetics and mechanism of cationic methyl violet and methylene blue dyes onto sepiolite, Dyes and Pigments, 75 (2007) 701-713.

[42] C. Gruian, E. Vanea, S. Simon, V. Simon, FTIR and XPS studies of protein adsorption onto functionalized bioactive glass, Biochimica et Biophysica Acta (BBA) - Proteins and Proteomics, 1824 (2012) 873-881.

[43] D.E. Giles, M. Mohapatra, T.B. Issa, S. Anand, P. Singh, Iron and aluminium based adsorption strategies for removing arsenic from water, Journal of Environmental Management, 92 (2011) 3011-3022.

[44] A.B. Albadarin, C. Mangwandi, A.a.H. Al-Muhtaseb, G.M. Walker, S.J. Allen, M.N.M. Ahmad, Kinetic and thermodynamics of chromium ions adsorption onto low-cost dolomite adsorbent, Chemical Engineering Journal, 179 (2012) 193-202.

[45] J. Liu, L. Wan, L. Zhang, Q. Zhou, Effect of pH, ionic strength, and temperature on the phosphate adsorption onto lanthanum-doped activated carbon fiber, Journal of Colloid and Interface Science, 364 (2011) 490-496.

[46] P. Ning, H.J. Bart, B. Li, X. Lu, Y. Zhang, Phosphate removal from wastewater by model-La(III) zeolite adsorbents, Journal of Environmental Sciences, 20 (2008) 670-674.

[47] L. Ding, C. Wu, H. Deng, X. Zhang, Adsorptive characteristics of phosphate from aqueous solutions by MIEX resin, Journal of Colloid and Interface Science, 376 (2012) 224-232.

[48] L. Zhang, Q. Zhou, J. Liu, N. Chang, L. Wan, J. Chen, Phosphate adsorption on lanthanum hydroxide-doped activated carbon fiber, Chemical Engineering Journal, 185–186 (2012) 160-167.

[49] H. Wu, D. Jiang, P. Cai, X. Rong, Q. Huang, Effects of low-molecular-weight organic ligands and phosphate on adsorption of Pseudomonas putida by clay minerals and iron oxide, Colloids and Surfaces B: Biointerfaces, 82 (2011) 147-151.

[50] E.I. Unuabonah, K.O. Adebowale, B.I. Olu-Owolabi, Kinetic and thermodynamic studies of the adsorption of lead (II) ions onto phosphate-modified kaolinite clay, Journal of Hazardous Materials, 144 (2007) 386-395.

[51] B.I. Olu-Owolabi, E.I. Unuabonah, Kinetic and thermodynamics of the removal of Zn^{2+} and Cu^{2+} from aqueous solution by sulphate and phosphate-modified Bentonite clay, Journal of Hazardous Materials, 184 (2010) 731-738.

[52] M. Özacar, Adsorption of phosphate from aqueous solution onto alunite, Chemosphere, 51 (2003) 321-327.

[53] H. Ye, F. Chen, Y. Sheng, G. Sheng, J. Fu, Adsorption of phosphate from aqueous solution onto modified palygorskites, Separation and Purification Technology, 50 (2006) 283-290.

[54] F. Haghseresht, S. Wang, D.D. Do, A novel lanthanum-modified bentonite, Phoslock, for phosphate removal from wastewaters, Applied Clay Science, 46 (2009) 369-375.

[55] B. Nowack, A.T. Stone, Competitive adsorption of phosphate and phosphonates onto goethite, Water Research, 40 (2006) 2201-2209.

[56] S. Chen, X. Chen, Y. Peng, K. Peng, A mathematical model of the effect of nitrogen and phosphorus on the growth of blue-green algae population, Applied Mathematical Modelling, 33 (2009) 1097-1106.

[57] J. Xiong, Y. Qin, E. Islam, M. Yue, W. Wang, Phosphate removal from solution using powdered freshwater mussel shells, Desalination, 276 (2011) 317-321.

[58] J. Gao, Z. Xiong, J. Zhang, W. Zhang, F. Obono Mba, Phosphorus removal from water of eutrophic Lake Donghu by five submerged macrophytes, Desalination, 242 (2009) 193-204.

[59] X. Jin, S. Wang, Y. Pang, H. Zhao, X. Zhou, The adsorption of phosphate on different trophic lake sediments, Colloids and Surfaces A: Physicochemical and Engineering Aspects, 254 (2005) 241-248.

[60] E.N. Peleka, E.A. Deliyanni, Adsorptive removal of phosphates from aqueous solutions, Desalination, 245 (2009) 357-371.

[61] B.K. Biswas, K. Inoue, K.N. Ghimire, S. Ohta, H. Harada, K. Ohto, H. Kawakita, The adsorption of phosphate from an aquatic environment using metal-loaded orange waste, Journal of Colloid and Interface Science, 312 (2007) 214-223.

[62] M. Yuan, W.W. Carmichael, E.D. Hilborn, Microcystin analysis in human sera and liver from human fatalities in Caruaru, Toxicon, 48 (2006) 627-640.

[63] I. Katz, C.G. Dosoretz, Desalination of domestic wastewater effluents: phosphate removal as pretreatment, Desalination, 222 (2008) 230-242.

[64] E. Vaiopoulou, P. Melidis, A. Aivasidis, Growth of filamentous bacteria in an enhanced biological phosphorus removal system, Desalination, 213 (2007) 288-296.

[65] L. Ruixia, G. Jinlong, T. Hongxiao, Adsorption of fluoride, phosphate, and arsenate ions on a new type of ion exchange fiber, Journal of Colloid and Interface Science, 248 (2002) 268-274.

[66] E.C. Moreno, K. Varughese, Crystal growth of calcium apatites from dilute solutions, Journal of Crystal Growth, 53 (1981) 20-30.

[67] J.B. Xiong, Q. Mahmood, Adsorptive removal of phosphate from aqueous media by peat, Desalination, 259 (2010) 59-64.

[68] S. Mohanty, J. Pradhan, S.N. Das, R.S. Thakur, Removal of phosphorus from aqueous solution using alumized red mud, International Journal of Environmental Studies, 61 (2004) 687-697.

[69] Z.Z. Ismail, Kinetic study for phosphate removal from water by recycled date-palm wastes as agricultural by-products, International Journal of Environmental Studies, 69 (2012) 135-149.

[70] N. Chen, Z. Zhang, C. Feng, M. Li, R. Chen, N. Sugiura, Investigations on the batch and fixed-bed column performance of fluoride adsorption by Kanuma mud, Desalination, 268 (2011) 76-82.

[71] APHA, AWWA, WPCF, Standard Methods for the Examination of Water and Wastewater, American Public Health Association, 20th ed (1999).

[72] D. Wu, B. Zhang, C. Li, Z. Zhang, H. Kong, Simultaneous removal of ammonium and phosphate by zeolite synthesized from fly ash as influenced by salt treatment, Journal of Colloid and Interface Science, 304 (2006) 300-306.

[73] J. Rouquérol, D. Avnir, C.W. Fairbridge, D.H. Everett, J.H. Haynes, N. Pericone, J.D.F. Ramsay, K.S.W. Sing, K.K. Unger, Recommendations for the characterization of porous solids, Pure and Applied Chemistry, 66 (1994) 1739-1759.

[74] J. Xiong, Z. He, Q. Mahmood, D. Liu, X. Yang, E. Islam, Phosphate removal from solution using steel slag through magnetic separation, Journal of Hazardous Materials, 152 (2008) 211-215.

[75] J. Su, H.G. Huang, X.Y. Jin, X.Q. Lu, Z.L. Chen, Synthesis, characterization and kinetic of a surfactant-modified bentonite used to remove As(III) and As(V) from aqueous solution, Journal of Hazardous Materials, 185 (2011) 63-70.

[76] W. Huang, S. Wang, Z. Zhu, L. Li, X. Yao, V. Rudolph, F. Haghseresht, Phosphate removal from wastewater using red mud, Journal of Hazardous Materials, 158 (2008) 35-42.

[77] X. Yang, B. Al-Duri, Kinetic modeling of liquid-phase adsorption of reactive dyes on activated carbon, Journal of Colloid and Interface Science, 287 (2005) 25-34.

[78] Y. Zhao, L.Y. Zhang, F. Ni, B. Xi, X. Xia, X. Peng, Z. Luan, Evaluation of a novel composite inorganic coagulant prepared by red mud for phosphate removal, Desalination, 273 (2011) 414-420.

[79] X. Huang, Intersection of isotherms for phosphate adsorption on hematite, Journal of Colloid and Interface Science, 271 (2004) 296-307.

[80] X. Yang, D. Wang, Z. Sun, H. Tang, Adsorption of phosphate at the aluminum (hydr)oxides–water interface: Role of the surface acid–base properties, Colloids and Surfaces A: Physicochemical and Engineering Aspects, 297 (2007) 84-90.

[81] C.R. Collins, K.V. Ragnarsdottir, D.M. Sherman, Effect of inorganic and organic ligands on the mechanism of cadmium sorption to goethite, Geochimica et Cosmochimica Acta, 63 (1999) 2989-3002.

[82] Y. Xue, H. Hou, S. Zhu, Characteristics and mechanisms of phosphate adsorption onto basic oxygen furnace slag, Journal of Hazardous Materials, 162 (2009) 973-980.

[83] M. Özacar, Phosphate adsorption characteristics of alunite to be used as a cement additive, Cement and Concrete Research, 33 (2003) 1583-1587.

[84] A. Ugurlu, B. Salman, Phosphorus removal by fly ash, Environment International, 24 (1998) 911-918.

[85] V.Z. Antonopoulos, S.K. Gianniou, Simulation of water temperature and dissolved oxygen distribution in Lake Vegoritis, Ecological Modelling, 160 (2003) 39-53.

[86] V.H. Smith, Eutrophication, Encyclopedia of Inland Waters, (2009) 61-73.

[87] V. Vyhnâlek, Lake restoration by reduction of nutrient loading. expectations, experiences, extrapolations. Internationale Revue der gesamten Hydrobiologie und Hydrographie, 76 (1991) 286-286.

[88] J. Heisler, P.M. Glibert, J.M. Burkholder, D.M. Anderson, W. Cochlan, W.C. Dennison, Q. Dortch, C.J. Gobler, C.A. Heil, E. Humphries, A. Lewitus, R. Magnien, H.G. Marshall, K. Sellner, D.A. Stockwell, D.K. Stoecker, M. Suddleson, Eutrophication and harmful algal blooms: A scientific consensus, Harmful Algae, 8 (2008) 3-13.

[89] H.P. Weikard, D. Seyhan, Distribution of phosphorus resources between rich and poor countries: The effect of recycling, Ecological Economics, 68 (2009) 1749-1755.

[90] L. Jing, X. Qin, Y. Luan, Y. Qu, M. Xie, Synthesis of efficient TiO_2-based photocatalysts by phosphate surface modification and the activity-enhanced mechanisms, Applied Surface Science, 258 (2012) 3340-3349.

[91] A. Roguska, S. Hiromoto, A. Yamamoto, M.J. Woźniak, M. Pisarek, M. Lewandowska, Collagen immobilization on 316L stainless steel surface with cathodic deposition of calcium phosphate, Applied Surface Science, 257 (2011) 5037-5045.

[92] F. Lusquiños, J. Pou, M. Boutinguiza, F. Quintero, R. Soto, B. León, M. Pérez-Amor, Main characteristics of calcium phosphate coatings obtained by laser cladding, Applied Surface Science, 247 (2005) 486-492.

[93] D. Cordell, J.O. Drangert, S. White, The story of phosphorus: Global food security and food for thought, Global Environmental Change, 19 (2009) 292-305.

[94] C.J. Liu, Y.Z. Li, Z.K. Luan, Z.Y. Chen, Z.G. Zhang, Z.P. Jia, Adsorption removal of phosphate from aqueous solution by active red mud, Journal of Environmental Sciences, 19 (2007) 1166-1170.

[95] X. Song, Y. Pan, Q. Wu, Z. Cheng, W. Ma, Phosphate removal from aqueous solutions by adsorption using ferric sludge, Desalination, 280 (2011) 384-390.

[96] D.E. Yates, T.W. Healy, Mechanism of anion adsorption at the ferric and chromic oxide/water interfaces, Journal of Colloid and Interface Science, 52 (1975) 222-228.

[97] K. Karageorgiou, M. Paschalis, G.N. Anastassakis, Removal of phosphate species from solution by adsorption onto calcite used as natural adsorbent, Journal of Hazardous Materials, 139 (2007) 447-452.

[98] B.B. Johnson, A.V. Ivanov, O.N. Antzutkin, W. Forsling, 31P nuclear magnetic resonance study of the adsorption of phosphate and phenyl phosphates on γ-Al_2O_3, Langmuir, 18 (2002) 1104-1111.

[99] L. Yan, Y. Xu, H. Yu, X. Xin, Q. Wei, B. Du, Adsorption of phosphate from aqueous solution by hydroxy-aluminum, hydroxy-iron and hydroxy-iron–aluminum pillared bentonites, Journal of Hazardous Materials, 179 (2010) 244-250.

[100] I. Fox, M.A. Malati, R. Perry, The adsorption and release of phosphate from sediments of a river receiving sewage effluent, Water Research, 23 (1989) 725-732.

[101] L. Zhu, R. Zhu, Simultaneous sorption of organic compounds and phosphate to inorganic–organic bentonites from water, Separation and Purification Technology, 54 (2007) 71-76.

[102] N. Chen, Z. Zhang, C. Feng, M. Li, D. Zhu, N. Sugiura, Studies on fluoride adsorption of iron-impregnated granular ceramics from aqueous solution, Materials Chemistry and Physics, 125 (2011) 293-298.

[103] L.A. Rodrigues, M.L.C.P. da Silva, Thermodynamic and kinetic investigations of phosphate adsorption onto hydrous niobium oxide prepared by homogeneous solution method, Desalination, 263 (2010) 29-35.

[104] S. Benyoucef, M. Amrani, Adsorption of phosphate ions onto low cost Aleppo pine adsorbent, Desalination, 275 (2011) 231-236.

[105] D.S. Bhargava, S.B. Sheldarkar, Use of TNSAC in phosphate adsorption studies and relationships. Effects of adsorption operating variables and related relationships, Water Research, 27 (1993) 313-324.

[106] R. Chitrakar, S. Tezuka, A. Sonoda, K. Sakane, K. Ooi, T. Hirotsu, Phosphate adsorption on synthetic goethite and akaganeite, Journal of Colloid and Interface Science, 298 (2006) 602-608.

[107] V. Istvánovics, Eutrophication of lakes and reservoirs, Encyclopedia of Inland Waters, (2009) 157-165.

[108] P. Ekholm, J. Lehtoranta, Does control of soil erosion inhibit aquatic eutrophication?, Journal of Environmental Management, 93 (2012) 140-146.

[109] L.E. de-Bashan, Y. Bashan, Recent advances in removing phosphorus from wastewater and its future use as fertilizer (1997–2003), Water Research, 38 (2004) 4222-4246.

[110] E. Lacasa, P. Cañizares, C. Sáez, F.J. Fernández, M.A. Rodrigo, Electrochemical phosphates removal using iron and aluminium electrodes, Chemical Engineering Journal, 172 (2011) 137-143.

[111] H.G. Kim, H.N. Jang, H.M. Kim, D.S. Lee, T.H. Chung, Effect of an electro phosphorous removal process on phosphorous removal and membrane permeability in a pilot-scale MBR, Desalination, 250 (2010) 629-633.

[112] N. Bektaş, H. Akbulut, H. Inan, A. Dimoglo, Removal of phosphate from aqueous solutions by electro-coagulation, Journal of Hazardous Materials, 106 (2004) 101-105.

[113] M.R. Awual, A. Jyo, T. Ihara, N. Seko, M. Tamada, K.T. Lim, Enhanced trace phosphate removal from water by zirconium(IV) loaded fibrous adsorbent, Water Research, 45 (2011) 4592-4600.

[114] Ş. İrdemez, N. Demircioğlu, Y.Ş. Yildiz, The effects of pH on phosphate removal from wastewater by electrocoagulation with iron plate electrodes, Journal of Hazardous Materials, 137 (2006) 1231-1235.

[115] J. Dai, H. Yang, H. Yan, Y. Shangguan, Q. Zheng, R. Cheng, Phosphate adsorption from aqueous solutions by disused adsorbents: Chitosan hydrogel beads after the removal of copper(II), Chemical Engineering Journal, 166 (2011) 970-977.

[116] S.I. Lyubchik, A.I. Lyubchik, O.L. Galushko, L.P. Tikhonova, J. Vital, I.M. Fonseca, S.B. Lyubchik, Kinetics and thermodynamics of the Cr(III) adsorption on the activated carbon from co-mingled wastes, Colloids and Surfaces A: Physicochemical and Engineering Aspects, 242 (2004) 151-158.

[117] T. Sangvanich, V. Sukwarotwat, R.J. Wiacek, R.M. Grudzien, G.E. Fryxell, R.S. Addleman, C. Timchalk, W. Yantasee, Selective capture of cesium and thallium from natural waters and simulated wastes with copper ferrocyanide functionalized mesoporous silica, Journal of Hazardous Materials, 182 (2010) 225-231.

Acknowledgements

I wish to express my sincere appreciation to my academic advisor, Professor Zhenya Zhang, for his guidance, encouragement and friendship during my studies at Tsukuba. His professionalism is an excellent example I can follow throughout my career.

I also would like to express my great appreciation to my dissertation committee members, Associate Professor Yingnan Yang, Zhongfang Lei and Motoo Utsumi for their numerous suggestion, comments, willingness and helpful discussion to serve as my advisory committee members.

Many friends and fellow students deserve recognition for their direct and indirect contributions to this dissertation. I wish to express my appreciation to the Miao Li, Yingxin Zhao, Dahu Ding, Wenli Huang, Yaning Wang, Chunguang Liu and many others for their countless assistance during the years of my study here.

I reserve much of my appreciation for my family. This dissertation would not have been completed without their love and support.

Finally, I would like to truthfully thank my girlfriend Shan Xie; this thesis cannot be finished without you, always appreciated.

This dissertation is dedicated to the people of the world who have devoted their lives to the protection of our environment.